

**TWO POTASSIUM CHANNELS IN THE PRESYNAPTIC AND
POSTSYNAPTIC COMPONENTS OF A SYNAPSE**

AN ABSTRACT

SUBMITTED ON THE FIFTEENTH DAY OF MARCH 2018
TO THE DEPARTMENT OF CELL & MOLECULAR BIOLOGY
IN PARTIAL FULFILLMENT OF THE REQUIREMENTS
OF THE SCHOOL OF SCIENCE AND ENGINEERING

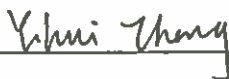
OF TULANE UNIVERSITY

FOR THE DEGREE

OF

DOCTOR OF PHILOSOPHY

BY



Yihui Zhang

Approved: 

Hai Huang, Ph.D.

Advisor



Jeffrey Tasker, Ph.D.



Ricardo Mostany, Ph.D.



Andrei Derbenev, Ph.D.

ABSTRACT

Reliable and precise signal transmission is essential in circuits of the auditory brainstem to encode timing with sub-millisecond accuracy. Globular bushy cells reliably and faithfully transfer spike signals to the principal neurons of the medial nucleus of the trapezoid body (MNTB) through calyx of Held, a giant glutamatergic synapse. Therefore, the MNTB works as a relay nucleus that preserves the temporal pattern of firing at high frequency. Using whole-cell patch-clamp recordings, we investigated the K^+ channels that shape the reliability of signal transfer across the rat calyx-MNTB synapse.

We observed that small-conductance calcium-activated potassium (SK) channels are expressed in the postsynaptic MNTB neurons. SK channels were activated by intracellular Ca^{2+} sparks and mediated spontaneous transient outward currents in developing MNTB neurons. SK channels were also activated by Ca^{2+} influx through voltage-gated Ca^{2+} channels and synaptically activated by NMDA receptors. Blocking SK channels with apamin depolarized the resting membrane potential, reduced resting conductance, and affected the responsiveness of MNTB neurons to signal inputs. Moreover, SK channels were activated by action potentials and affected the spike afterhyperpolarization. Blocking SK channels disrupted the one-to-one signal transmission from presynaptic calyces to postsynaptic MNTB neurons and induced extra postsynaptic action potentials in response to presynaptic firing.

KCNQ channels are slow-activating and non-inactivating, voltage-gated K^+ channels. In addition to controlling the resting properties of the presynaptic calyceal terminal, we found that KCNQ channels were cumulatively activated during high-frequency firing and contributed to maintaining the normal presynaptic action potential waveform. Blocking KCNQ channels led to the cumulative inactivation of presynaptic Na^+ and Kv1 channels, and disrupted the reliable action potential waveform and calcium influx required for reliable synaptic transmission.

These data reveal that both postsynaptic SK channels and presynaptic KCNQ channels play important roles in regulating electrical activity and are crucial for reliable high-frequency signal transmission across the calyx-MNTB synapse.

**TWO POTASSIUM CHANNELS IN THE PRESYNAPTIC AND
POSTSYNAPTIC COMPONENTS OF A SYNAPSE**

A DISSERTATION

SUBMITTED ON THE FIFTEENTH DAY OF MARCH 2018
TO THE DEPARTMENT OF CELL & MOLECULAR BIOLOGY
IN PARTIAL FULFILLMENT OF THE REQUIREMENTS
OF THE SCHOOL OF SCIENCE AND ENGINEERING

OF TULANE UNIVERSITY

FOR THE DEGREE

OF

DOCTOR OF PHILOSOPHY

BY

Yihui Zhang.

Yihui Zhang

Approved: _____

Haitt

Hai Huang, Ph.D.

Advisor

Jeffrey Tasker, Ph.D.

Jeffrey Tasker

Ricardo Mostany, Ph.D.

Andrew Derbenev, Ph.D.

©Copyright by Yihui Zhang, 2018

All Rights Reserved

ACKNOWLEDGEMENTS

First and foremost I want to express my sincere gratitude to my advisor Dr. Hai Huang, for his patient guidance and consistent support throughout all these years. Thank Dr.Huang for giving me the opportunity to work in his lab. Without his continuous contribution of time, idea and funding to my projects, there is no way that I could be able to make it such far in this long and tough journey, and eventually to a successful end now.

At the same time, I would like to thank my committee members, Dr. Jeffrey Tasker, Dr. Ricardo Mostany, and Dr. Andrei Derbenev for their helpful advice for my research over all these years. Their academic support, constructive criticism, and valuable guidance helped me progress towards the completion of my graduate study. Special thanks also go to Dr. Benjamin Hall for his great support when I was in his lab, and to Dr. Laura Schrader who offered a lot of helpful suggestions for my latest publication that is a part of my thesis work.

I enjoyed a lot working in Dr. Huang's lab. First, I want to express my thanks to Dainan Li for all meaningful discussion about projects and experiments. I would like to thank Yun Zhu for his assistance in some of my experiments. I would also like to thank Youad Darwish for revising my latest published paper .

I also want to express my thanks to the people in the basement. Special thanks go to the previous members in Dr. Hall's lab, Dr. Oliver Miller, Dr. Chih-Chieh Wang and Dr. Jacqueline Moran for their kind help when I was working in Dr. Hall's lab. I also want to thank great people from Tasker lab, especially Dr. Shi Di who gave me a lot of advice and encouragement for my career and life, and also Dr. Zhiying Jiang who introduced me to the field of electrophysiology hand by hand.

I would also like to thank the nice people in CMB office, Marnie Mercado, John Drwiega, Jonathan Flack and Haini Yu for their assistance for our daily work.

Special thanks go to Dr. Wen Han and Dr. Fading Chen. They always support and encourage me especially when I felt lost in my research and life. The time that I spent with them in my Ph.D. career will definitely become a wonderful memory for the rest of my life. It is hard to imagine a life without them being around all these years.

Last but not the least I would like to thank my parents and family, for their unconditional understanding and support to allow me to pursue my scientific dream. Their love and encouragement have given me the strength and energy to finish my Ph.D. career.

TABLE OF CONTENTS

| | |
|---------------------------------------------------------------------------------|-----------|
| ACKNOWLEDGEMENTS | ii |
| CHAPTER 1. INTRODUCTION | 1 |
| 1.1 Overview | 1 |
| 1.2 MNTB..... | 3 |
| 1.2.1 Circuitry of the MNTB..... | 3 |
| 1.2.2 Function of the MNTB..... | 3 |
| 1.3 Development and topology of MNTB | 5 |
| 1.3.1 Developmental change of MNTB..... | 5 |
| 1.3.2 Topographic organization of MNTB..... | 6 |
| 1.4 Calyx-MNTB synapse..... | 7 |
| 1.4.1 Calyx of Held | 7 |
| 1.4.2 Principal MNTB neuron | 10 |
| 1.4.3 Signal transmission between calyx of Held and MNTB neuron | 11 |
| 1.5 K⁺ channels: focus on SK channels and KCNQ channels. | 13 |
| 1.5.1 Overview | 13 |

| | | |
|-------------------------------------------------------------------------------------------------------------------------------|----------------------------------------------------------------------------|-----------|
| 1.5.2 | SK channels | 13 |
| 1.5.3 | KCNQ channels..... | 15 |
| 1.6 | Aims of the study..... | 17 |
| CHAPTER 2. MATERIALS AND METHODS..... | | 19 |
| 2.1 | Slice preparation | 19 |
| 2.2 | Whole-cell recordings | 22 |
| 2.3 | Drugs | 27 |
| 2.4 | Analysis | 27 |
| CHAPTER 3. SK CHANNELS REGULATE RESTING PROPERTIES AND SIGNALING RELIABILITY OF A DEVELOPING FAST SPIKING NEURON | | 29 |
| 3.1 | Abstract..... | 29 |
| 3.2 | Results | 32 |
| 3.2.1 | A spontaneous transient outward current mediated by SK channels.. | 32 |
| 3.2.2 | Activation of tonic SK Current..... | 40 |
| 3.2.3 | SK channels contribute to resting membrane potential and conductance | 45 |

| | |
|-------------------------------------------------------------------------------------------|-----------|
| 3.2.4 SK currents modulate signal responsiveness..... | 47 |
| 3.2.5 Activation of SK channels by NMDA receptors..... | 47 |
| 3.2.6 Activation of SK channels during action potential | 52 |
| 3.2.7 SK currents regulate reliability of signal transmission | 52 |
| 3.3 Discussion | 57 |
| 3.3.1 Activation of SK channels at MNTB neurons | 57 |
| 3.3.2 SK channels and membrane properties | 59 |
| 3.3.3 SK channels subserve auditory function..... | 60 |
| CHAPTER 4. KCNQ CHANNELS REGULATE FIRING PROPERTIES OF THE CALYX OF HELD | 63 |
| 4.1 Abstract..... | 63 |
| 4.2 Results | 64 |
| 4.2.1 KCNQ channels regulate the terminal excitability..... | 64 |
| 4.2.2 Lack of activity-dependent AP broadening in calyx of Held | 68 |
| 4.2.3 KCNQ contributes to maintaining AP waveform during high-frequency firing..... | 71 |

| | |
|-----------------------------------------------------------------------------------------------------------------------------------|-----------|
| 4.2.4 KCNQ prevents the accumulative inactivation of Na ⁺ and Kv1 channels in calyx during high-frequency firing | 75 |
| 4.2.5 KCNQ channels interact with Na ⁺ and Kv1 channels to regulate the waveform of AP | 81 |
| 4.2.6 Function of KCNQ channels in regulating calcium response during high-frequency firing | 83 |
| 4.3 Discussion | 87 |
| 4.3.1 KCNQ channels affect the presynaptic terminal excitability | 87 |
| 4.3.2 KCNQ is important for constant AP waveform of calyx during high-frequency firing..... | 88 |
| 4.3.3 Impact of AP waveforms on calcium influx during high-frequency firing | 91 |
| CHAPTER 5. CONCLUSION AND PERSPECTIVES | 94 |
| 5.1 Conclusion | 94 |
| 5.2 Future perspectives..... | 96 |
| 5.2.1 The physiological function of STOCs..... | 96 |
| 5.2.2 Role of presynaptic KCNQ channels in the conventional synapse..... | 98 |
| 5.2.3 Diseases related to SK channels and KCNQ channels | 99 |

| | |
|------------------------|------------|
| REFERENCES..... | 101 |
| BIOGRAPHY | 118 |

LIST OF TABLES

| | |
|------------------------------------------------------------------------------------|-----------|
| Table 2.1 Saline for slicing. | 20 |
| Table 2.2 The aCSF for incubation and recording. | 21 |
| Table 2.3 Post- and Pre- synaptic pipette solutions. | 24 |
| Table 2.4 Pipette solution for AMPA receptor-mediated EPSC recordings. | 25 |
| Table 2.5 Pipette solution for examining sodium current. | 26 |
| Table 2.6 Drugs and suppliers. | 28 |

LIST OF FIGURES

| | |
|-------------------------------------------------------------------------------------------------------------|-----------|
| Figure 3. 1. SK channels mediated STOCs..... | 35 |
| Figure 3. 2. Development change of STOCs..... | 37 |
| Figure 3. 3. Calcium sparks activated the transient SK current. | 38 |
| Figure 3. 4. Tonic SK current. | 42 |
| Figure 3. 5. Activation of SK current..... | 44 |
| Figure 3. 6. Effects of SK channels on resting membrane properties of MNTB neurons..... | 46 |
| Figure 3. 7. Effects of SK channels on the responsiveness. | 49 |
| Figure 3. 8. Activation of SK channels by Ca²⁺ influx through NMDA receptors. | 50 |
| Figure 3. 9. Activation of SK channels during the action potential. | 54 |
| Figure 3. 10. SK channel activation was required for highly reliable signal transmission..... | 55 |
| Figure 4. 1. KCNQ channels regulate the excitability of calyx of Held. | 66 |
| Figure 4. 2. Minimum AP waveform change during high-frequency AP activity in calyx of Held..... | 69 |
| Figure 4. 3. KCNQ regulates the shape of APs during high-frequency AP activity in calyx of Held..... | 73 |

| | |
|----------------------------------------------------------------------------------------------------------------------|-----------|
| Figure 4. 4. KCNQ inhibits accumulative inactivation of Na⁺ channels at high-frequency firing..... | 77 |
| Figure 4. 5. KCNQ prevents the accumulative inactivation of Kv1, but not Kv3, at high-frequency firing..... | 79 |
| Figure 4. 6. KCNQ interacts with NaV and Kv1 channels to regulate the AP waveform. | 82 |
| Figure 4. 7. Functions of KCNQ affect calcium currents during high-frequency AP activity..... | 85 |

CHAPTER 1. INTRODUCTION

1.1 Overview

Synapses are highly specialized structures that mediate interaction and communication between neurons. In average, a human brain is composed of approximately 100 to 500 trillion synapses for about 86 billion neurons (Azevedo et al., 2009). In general, a synapse in central nervous system (CNS) consists of 3 basic components: 1) a presynaptic element, usually an axon terminal, 2) a synaptic cleft, and 3) a postsynaptic element. These chemical synapses can be categorized by the nature of different neurotransmitters released from presynaptic terminals. Activation of an excitatory synapse, commonly triggered by glutamate, depolarizes neuronal cell membrane, while on the other hand, an inhibitory synapse utilizes its neurotransmitter, likely GABA or Glycine, to produce an opposite effect, hyperpolarizing neuronal cell membrane (Deutch, 2013). Neurons receive both synaptic inputs simultaneously, which subsequently alter neuron resting membrane potential (RMP) that is typically around -70 mV. Under certain circumstance, summation of excitatory synaptic inputs brings neuron RMP closer to its threshold to generate an action potential (AP) at the initial segment, from which it propagates along the axon to axon terminals, triggering the releasing of different neurotransmitters (McCormick, 2013).

To ensure accuracy, reliable and precise signal transmission across synapses is essential for synaptic transmission, especially for fast-spiking neurons. It has been documented that both presynaptic and postsynaptic mechanisms contribute to the reliability of synaptic transmission, however, the exact mechanism is not fully addressed, partially due to the technical difficulty to record directly from synaptic terminals in conventional synapses using classic electrophysiological techniques.

The calyx of Held is one of the largest synapses in the mammalian brain. In postnatal day 9 (P9) mice, the area of the calyceal membrane is $\sim 2500 \mu\text{m}^2$, and the volume is $\sim 480 \mu\text{m}^3$ (Sätzler et al., 2002). Its giant size allows electrophysiologists to conduct direct patch-clamp recordings from both the presynaptic terminal and its postsynaptic partner, the MNTB neuron. The calyx-MNTB synapse has been extensively studied and is an established model system for investigating voltage-gated ion channels of presynaptic terminals and fast glutamatergic neurotransmission (Ryugo and Spirou, 2010; Schneggenburger and Forsythe, 2006). Furthermore, the calyx-MNTB synapse is a component of the inverting relay pathway in the auditory system, processing important information for sound localization. In this thesis, I examined two essential potassium channels in the calyx-MNTB synapses: SK channels in the MNTB neuron and KCNQ channels in the calyx of Held. I investigated how they regulate the synaptic properties and neurotransmission in calyx-MNTB synapses with their different localizations and revealed their profound roles in the auditory system. My data also provide considerable insight into their potential functions in conventional synapses.

1.2 MNTB

1.2.1 Circuitry of the MNTB

The MNTB is one of the nuclei in the superior olivary complex (SOC) localizing in the auditory brainstem. The prominent excitatory inputs for MNTB neurons originate from the contralateral anteroventral cochlear nucleus (AVCN). One single axon from the globular bushy cell (GBC) of contralateral AVCN forms one single axon terminal, calyx of Held, connecting with one target principal neuron in MNTB. The MNTB also receives a few excitatory inputs from the contralateral posteroventral cochlear nucleus (PVCN) and some other noncalyceal excitatory inputs with unclear origin (Borst and Soria van Hoeve, 2012; Hamann et al., 2003). The inhibitory inputs of MNTB originate from the contralateral and ipsilateral lateral nucleus of the trapezoid body (LNTB) and ventral nucleus of the trapezoid body (VNTB) (Burger et al., 2015).

Principal neurons in the MNTB form inhibitory synapses at multiple targets in the SOC. The main projections of MNTB neurons are ipsilateral lateral superior olive (LSO) and superior paraolivary nucleus (SPON) (Borst and Soria van Hoeve, 2012). Additionally, research has found that MNTB neurons also project to medial superior olive (MSO) (Grothe, 2003; Schneggenburger and Forsythe, 2006).

1.2.2 Function of the MNTB

The primary function of the MNTB is to participate in computing the spatial location of sound sources. Since the MNTB neurons are driven by glutamatergic calyceal terminals to release glycine, MNTB serves as an inverting relay in the binaural auditory pathway to invert the contralateral excitatory signal to an inhibitory signal and to provide inhibition to the downstream nuclei in the SOC, which is the first stage of the auditory circuit to compute the sound localization. The MNTB provides the critical information for interaural time difference (ITD) and interaural intensity difference (IID) through inhibiting different downstream nuclei.

The LSO is the main projection of the MNTB, and it is the first site of the auditory circuit for computing IID, which is a significant source of information used to localize high-frequency sounds. The LSO also receives direct excitatory projection originating from the ipsilateral ear via the cochlear nucleus except for contralateral inhibition from the MNTB. The LSO integrates information by subtracting contralateral inhibition from the ipsilateral excitation (Boudreau and Tsuchitani, 1968). In addition to the LSO, another projection of MNTB – MSO is the first stage responsible for ITD processing. Low-frequency sounds are localized mainly based on ITD. The excitatory inputs of MSO originate from cochlear nuclei on both sides of the brainstem. Neurons in the MSO use the latency of arrivals of the two excitatory inputs to identify the difference in the arrival times of sounds at two ears. The inhibition from MNTB adjusts the temporal sensitivity of neurons in the MSO, but its ultimate function is not clear (Grothe, 2003).

Sound localization is essential for both the survival of mammalian animals from the hunting by predators, and the quality of life of humans. Multiple sclerosis (MS) and stroke patients with brainstem lesions involving the MNTB are reported to have impaired ability in sound localization (Furst et al., 2000). In the test of binaural

lateralization, these subjects show side-oriented performance, having trouble with discriminating test stimuli from the center position and tending to lateralize all test stimuli to one side or the other of the head.

1.3 Development and topology of MNTB

1.3.1 Developmental change of MNTB

The calyx-MNTB synapse is the largest synapse in the mammalian brain. In the rodent brain, the diameter of the MNTB neuron is approximately 15–20 μm . Each mature MNTB neuron is innervated by a single calyx. However, the shape of the calyx and its connection with the MNTB principal neuron undergo dramatic transition during development. The original contact between calyx and MNTB neurons starts to form at embryonic day 17 (E17) (Hoffpauir et al., 2010). Initial somatic contact then expands to form the protocalyx at P2 (Hoffpauir, 2006). During the early formation of the calyceal synapse, a single axon of GBC can branch and establish multiple connections with nearby principal neurons (Kuwabara et al., 1991; Rodríguez-Contreras et al., 2006). Also, more than half of the MNTB neurons receive multiple innervations from the cochlear nucleus during E18 to postnatal day 2 (P2). Striking changes were detected at P4. The protocalyx grows into an immature calyx, which is a cup-like structure that covers 40% of the surface area of the MNTB neuron (Sätzler et al., 2002). At this time, 85% of the MNTB neurons become mono-innervated by the immature calyceal terminals, and other superfluous connections disappear (Hoffpauir et al., 2010;

Nakamura and Cramer, 2011). Morphological transformations last several weeks. The calyx develops from the cup- to the finger-digit-like shape which is the adult morphology of the calyx (Ford et al., 2009; Kandler and Friauf, 1993). The multi-finger-like structure facilitates the rapid clearance of glutamate from the synaptic cleft, which might ensure the fast decay kinetics of the synaptic current and facilitate precise signal transmission.

1.3.2 Topographic organization of MNTB

With the maturation of the auditory system, the three-dimensional topographic organization of the MNTB is also established and reaches adult properties around P14 (Friauf, 1992). In general, MNTB is arranged in an orderly layout along the mediolateral axis. The principal neurons located medially within the nucleus receive inputs of high acoustic frequency, while the neurons located laterally receive inputs of low acoustic frequency (Kandler et al., 2009; Sonntag et al., 2009). To respond to inputs of different frequency along the mediolateral axis, neurons in the MNTB develop a topographic arrangement of firing properties and ion channel expression. For example, because of the higher expression level of high-voltage-activated Kv3.1 channels and hyperpolarization-activated cyclic nucleotide-gated (HCN) channels, the high-threshold K^+ conductance and hyperpolarization-activated currents are larger in medial than lateral neurons, which promote proper firing properties of the medial neurons in response to high-frequency tones. In contrast, the expression of low-voltage-activated Kv1.1 is significantly greater in lateral MNTB neurons (Leao et al., 2006). Spontaneous auditory nerve activity before hearing onset is essential for the tonotopic organization

of the MNTB (Clause et al., 2014). Impairment of prehearing spontaneous activities in deaf mice disrupts the normal topographic gradient of neuronal membrane properties in the MNTB (Leao et al., 2006).

1.4 Calyx-MNTB synapse

1.4.1 Calyx of Held

Accompanying the morphological maturity of the calyx during development, the shape of the action potential undergoes a distinguishing change, as well. The half-width of APs significantly shortens to less than 0.2 ms, while the amplitude of APs remains stable. (Taschenberger and von Gersdorff, 2000). A typical AP in the calyx exhibits an afterhyperpolarization succeeded by an afterdepolarization after maturation.

The calyx of Held has a specialized complement of voltage-gated ion channels to achieve briefer APs. First of all, the calyx expresses a high density of Na⁺ channels in the calyceal terminal and heminodes (Leão et al., 2005; Sierksma and Borst, 2017a; Xu et al., 2017). The subtype of Na⁺ channels in the calyx is Nav1.6 (Leão et al., 2005). Opening Na⁺ channels generate three different types of currents: transient, resurgent and persistent Na⁺ current in the calyx of Held. Transient Na⁺ current is activated during the depolarizing phase of the AP. It has a very fast rate of activation and inactivation which can be finished within 3 ms. Furthermore, the recovery from inactivation is rapid ($\tau = 2.4$ ms at $V = -80$ mV), which promotes the short AP shape (Leão et al., 2005). A resurgent Na⁺ current is generated at the repolarizing phase of an AP and plays an important role in regulating the depolarizing afterpotential (DAP) (Hee Kim et al.,

2010a). The calyx of Held is also expressed a persistent Na^+ current, which has an activation voltage of -85 mV (Huang and Trussell, 2008). Blockage of persistent Na^+ current affects the resting properties of calyceal terminals and their responses to glycine.

Voltage-gated K^+ channels also play essential roles in controlling the AP in the calyx. Based on the activation threshold, they can be divided into two types: low-threshold K^+ channels and high-threshold K^+ channels. In the calyx, low-threshold K^+ channels contain subtypes Kv1.1, Kv1.2, Kv1.3, and KCNQ channels. While Kv1.1 and Kv1.2 predominantly localize in the transition zone between axon and terminal, Kv1.3 is expressed in the terminal itself (Dodson et al., 2003; Gazula et al., 2010). The primary function of Kv1 channels in the calyx is to reduce the DAP amplitude and further prevent any aberrant firing. However, blockage of Kv1 with specific blocker margatoxin does not affect the AP waveform. However, Kv3, which belongs to the high-threshold K^+ channel, contributes to shaping the AP waveform by regulating the repolarization and limiting the AP duration (Ishikawa et al., 2003). Since Kv3 channels open only during strong depolarizing activity, such as an AP, without affecting spike initiation, they are also essential for facilitating high-frequency firing. Immunostaining reveals that Kv3 channels are present in the synaptic terminal of the calyx and that the main subtype is Kv3.1 (Dodson et al., 2003; Li et al., 2001; Puente et al., 2003).

Except for currents that are activated by depolarization of membrane potential, hyperpolarizing the membrane potential of the calyx can activate a non-specific cation current, I_h which is mediated by HCN channels in the calyx (Cuttle et al., 2001). The predominant role for I_h is to establish the resting membrane potential and to regulate the post-tetanic afterhyperpolarization (Kim et al., 2007a).

The presynaptic terminal AP provides a critical window of time for voltage-dependent Ca^{2+} channels (VGCCs) to be activated, which induces calcium influx and further triggers neurotransmitter release (Borst and Sakmann, 1996, 1998; Borst et al., 1995; Wu et al., 1999). Therefore, the shape of the AP plays a vital role in regulating the amount of calcium influx and further determining the timing and strength of synaptic transmission (Borst and Sakmann, 1999; Sabatini and Regehr, 1997; Yang, 2006a). Ion channels with the capability of sculpting the AP waveform have a profound effect on signal transmission across the synapse (Hee Kim et al., 2010a; Hori and Takahashi, 2009a; Ishikawa et al., 2003). At early development, multiple subtypes of VGCCs have been detected in the calyx, which includes N-type, R-type, and P/Q-type Ca^{2+} channels (Wu et al., 1998). Among these subtypes, P/Q-type of Ca^{2+} channels are the most effective in regulating the glutamate release. The specific blocker of P/Q-type Ca^{2+} channels, ω -agatoxin-IVA, was found to reduce the calcium influx about 70% and decreased the EPSC to 26% (Wu et al., 1999). There is a relatively greater distance of a substantial fraction of N-type and R-type Ca^{2+} channels from the release sites. Accordingly, the calcium influx through N-type and R-type Ca^{2+} channels is less effective in controlling glutamate release in the calyx (Inchauspe et al., 2007). The subtypes of VGCCs undergo a developmental switch with the morphological maturation of the calyx. P/Q-type Ca^{2+} channels gradually replace the N-type and R-type Ca^{2+} channels, and control almost all of the glutamate release in the calyx (Iwasaki and Takahashi, 1998a, 1998b).

The resting membrane potential of the calyx is typically around -70 mV to -80 mV (Forsythe, 1994). Generally, the ion channels involved in setting the RMP of a neuron include the inwardly rectifying potassium channels (Kir), the leak channels (K2p) and voltage-gated channels opening around the RMP (Johnston et al., 2010).

Among all the ion channels involved, the contribution of the voltage-gated channels in regulating the RMP is most extensively examined in the calyx. Voltage-gated channels have a relatively negative activation threshold such as persistent sodium channels, KCNQ channels, and HCN channels, contribute to mediate RMP. (Huang and Trussell, 2008, 2011; Kim et al., 2007b). Presynaptic RMP plays an important role in regulating the background calcium concentration and has a profound effect on the transmitter release. Depolarization of RMP facilitates transmitter release by promoting presynaptic calcium current (Hori and Takahashi, 2009a).

1.4.2 Principal MNTB neuron

Glutamates released from the calyx binds to the AMPA and NMDA receptors and induces APs in MNTB neurons (Forsythe and Barnes-Davies, 1993; Joshi, 2004; Joshi and Wang, 2002). Similar to the calyx of Held, MNTB neurons also express 1) Na⁺ channels with rapid recovery time from inactivation to maintain the short AP shape (Leão et al., 2005, 2008; Ming and Wang, 2003); 2) Kv1 channels to inhibit MNTB neuron from aberrant firing by shunting the DAP (Brew and Forsythe, 1995); 3) Kv3 potassium channels to regulate the firing pattern (Wang et al., 1998) and 4) P/Q-type, N-type, and R-type of Ca²⁺ channels to mediate glycine release. However, ion channels detected in the MNTB neurons are not exactly the same as in the calyx of Held. First of all, the subtypes of Kv1 channels localizing in the MNTB neurons are different from those in the calyx. Instead of Kv1.3, Kv1.6 is expressed in the soma, along with Kv1.1 and Kv1.2, which are in the somatic and axonal sites of MNTB neurons (Brew and Forsythe, 1995). Second, Kv2.2 channels have been detected in the axon initial segment

(AIS) of MNTB neurons, accelerating the AP repolarization and hyperpolarizing the inter-spike potential during high-frequency firing (Johnston et al., 2008). Third, L-type Ca^{2+} currents have been reported in MNTB neurons with unknown function (Barnes-Davies et al., 2001).

While most of the research has focused on the voltage-gated conductance during the action potentials, less attention has been paid to the resting conductance of MNTB neurons, which is mainly determined by a potassium-based leak conductance, K_{2p} . In addition to exerting a significant effect on regulating the resting membrane properties, it also influences the cell excitability and spike timing (Berntson and Walmsley, 2008).

1.4.3 Signal transmission between calyx of Held and MNTB neuron

In order to encode timing with sub-millisecond accuracy, the calyx-MNTB synapse can fire at a very high frequency. In physiological condition, the spontaneous firing rate of a single afferent fiber of MNTB in cats is between 10 to 150 Hz (Sierksma and Borst, 2017a; Spirou et al., 1990). In *in vivo* studies of mice, a developmental change in spontaneous firing rate was detected. At P8 to P9, the range of spontaneous firing is between 1 ~ 20 sp/s. After hearing onset, the upper limit further increases to around 200 sp/s. Acoustically driven responses have a range between 2 to 40 kHz (Sonntag et al., 2009). The refractory period following AP is critical for high-frequency firing. In the refractory period, the excitability of the membrane decreases, which effectively limits the generation of the next action potential. Two major determinants of the refractory period are the inactivation of Na^+ channels and the deactivation of K^+ channels (Bucher and Gozell, 2011).

In some terminals including hippocampal mossy fiber boutons (MFBs) and pituitary nerve terminals, long lasting, high-frequency firing can result in AP broadening due to the accumulative inactivation of Kv1 channels (Geiger and Jonas, 2000; Jackson et al., 1991). However, activity-dependent AP broadening was not observed in the calyx of Held. Mechanisms underlying the maintenance of the calyx AP stability during high-frequency firing are poorly understood.

Furthermore, the calyx-MNTB synapse is characterized by its high-fidelity signal transmission that preserves the temporal pattern of firing at high frequency (Laughlin et al., 2008; Lorteije et al., 2009; Taschenberger and von Gersdorff, 2000). Simple interpretation of the reliable synaptic transmission assumes that a presynaptic AP elicits a single postsynaptic spike. GBCs fire action potentials reliably and precisely synchronize to sound. For example, GBCs with the characteristic frequency of 700 Hz entrain to the sound and fire an action potential to every stimulus cycle with a phase locking value of 0.99 (Joris et al., 1994). Several cellular mechanisms have been established that are important to support neurotransmission at such high rates, including presynaptic ion channels that enable reliable presynaptic spike waveform and calcium influx; large readily releasable pool; many release sites; and low release probability that enhance the release reliability; as well as fast kinetics of postsynaptic AMPA-type glutamate receptors that allow fast and faithful transmission to the postsynaptic MNTB (Borst and Soria van Hoeve, 2012; Taschenberger and von Gersdorff, 2000; Taschenberger et al., 2002; Wu et al., 2009). Moreover, different voltage-gated K⁺ channels are expressed on the pre- and postsynaptic components to control neuronal excitability, determine spike shape, and enable high-frequency firing (Brew and Forsythe, 1995; Dodson et al., 2002; Huang and Trussell, 2011; Wang et al., 1998; Yang et al., 2014).

1.5 K⁺ channels: focus on SK channels and KCNQ channels.

1.5.1 Overview

K⁺ channels are the most diverse class of ion channels and exist in various types of cells such as neurons, cardiomyocytes, pancreatic β -cells, and many more. In humans, over 70 genes encode different types of K⁺ channels. In neurons, K⁺ channels actively participate in setting the resting membrane potential, shaping the AP waveform, and regulating firing frequency of APs. However, with their unique kinetics and properties, each of them plays multiple different roles in controlling neuronal features and electrical activities. Mutations in K⁺ channels have been implicated in several neurological diseases. For example, mutations in the human voltage-gated K⁺ channel gene Kv1.1 are related to episodic ataxia type 1 and partial epilepsy (Zuberi et al., 1999).

1.5.2 SK channels

Small conductance calcium-activated potassium (SK) channels belong to the subfamily of Ca²⁺-activated K⁺ channels and was first characterized in red blood cells in 1958 (GARDOS, 1958). It was called the small-conductance channels because compared to the big-conductance K⁺ (BK) channels that have a single channel conductance of 100-200 pS, SK channels have a relatively lower unit conductance value of 10-20 pS (Vergara et al., 1998). There are three different subtypes of SK

channels: $K_{Ca2.1}$ (SK1), $K_{Ca2.2}$ (SK2), and $K_{Ca2.3}$ (SK3) that are encoded by the genes *KCNN1*, *KCNN2*, and *KCNN3*, respectively. Four subunits assemble as a homomeric or heteromeric SK channel tetramer. Each subunit consists of six transmembrane (TM) domains and cytosolic N- and C-termini residing within the cytoplasm. The TM domain 5 and 6 of each subunit form the core of the SK channel (Maylie et al., 2004). SK channels are predominantly distributed in brain regions such as the neocortex, hippocampus, thalamus, and various brainstem nuclei. Each subunit has a different expression level in various brain regions. For example, in the layer V pyramidal neurons in the neocortex, SK1 and SK2 have higher expression level than SK3 (Sailer et al., 2004; Stocker and Pedarzani, 2000). A highly selective blocker of SK channels is apamin, and the SK channel is the only known target for apamin.

SK channels are voltage-independent channels that are activated by submicromolar concentrations of cytosolic Ca^{2+} with a half-maximal activation concentration of 0.1-1 μ M (Blatz and Magleby, 1986; Xia et al., 1998). Although the activation of SK channels by Ca^{2+} is rapid with activation time constants of 5-15 ms (Xia et al., 1998), SK channels do not contain direct intrinsic Ca^{2+} -binding motifs. Instead, Ca^{2+} gating is achieved by the constitutive association between the pore-forming subunits and calmodulin (Schumacher et al., 2001). To activate the SK channels, calcium first binds to the calmodulin and leads to the subsequent conformational change of the SK channels. Four major cytosolic calcium sources activate the SK channels: 1) Ca^{2+} influx via VGCCs; 2) Ca^{2+} influx via Ca^{2+} -permeable agonist-gated ion channels, such as NMDAR and nAChRs; 3) Ca^{2+} released from intracellular Ca^{2+} stores by generation of inositol trisphosphate (IP3) via G protein-coupled receptors, as well as the ryanodine receptor, and 4) Ca^{2+} -induced Ca^{2+} release (CICR) (Adelman et al., 2012a). Under resting membrane potential, however, the

cytosolic Ca^{2+} level is usually low, and SK channels are not active (Adelman et al., 2012b).

The Ca^{2+} -gated property couples the opening of SK channels with membrane potential. Activation of SK channels causes a change in cellular excitability. APs serve as important electrical activity within a neuron that promotes the opening of VGCCs and influx of Ca^{2+} , driving the opening of SK channels (Bevan and Wilson, 1999; Edgerton and Reinhart, 2003; Hallworth et al., 2003). As a result, SK channel activity is one of the major determinants of the AHP phase of APs, especially the medium (m) AHP, which activates rapidly and decays over several hundred milliseconds (Stocker et al., 1999).

SK channel activity is associated with synaptic plasticity and the regulation of learning and memory (Hammond, 2006; Kramar, 2004; Stackman et al., 2002). Blocking SK activity can facilitate the induction of synaptic plasticity and enhance hippocampal-dependent spatial learning and memory, while overexpression of SK channels in the hippocampus produces opposite effects. The activity of SK channels is related to diseases such as schizophrenia and Alzheimer's disease (Chandy et al., 1998; Ikonen and Riekkinen, 1999; Imbrici et al., 2013). In mouse models of Alzheimer's disease that exhibit cognitive deficits, impairments in the cholinergic excitation of layer six prefrontal neurons are associated with altered SK channels activity (Proulx et al., 2015).

1.5.3 KCNQ channels

Unlike SK channels, KCNQ channels are voltage-dependent K^+ channels that mediate a slow-activating delayed rectifier current (Delmas and Brown, 2005; Greene and Hoshi, 2017; Jentsch, 2000). Five Kv7 subtypes belong to this family – Kv7.1 to Kv7.5 (Jentsch, 2000). With the exception of Kv7.1, which is the predominant subunit found in heart and peripheral epithelial cells, as well as smooth muscle, Kv7.2–Kv7.5 are mainly expressed throughout the CNS in various types of neurons (Passmore et al., 2003; Sanguinetti et al., 1996; Yus-Nájera et al., 2003). The structure of KCNQ proteins is similar to other Kv proteins that contain 6 TM domains; a single P-loop that functions as the selectivity filter component of the pore, and a long C-terminal tail (Howard et al., 2007). They assemble as tetramers to form the functional KCNQ channels. KCNQ channels are the essential component of M-currents, which are so named because stimulation of muscarinic acetylcholine receptors (mAChR) suppressed this current at the time it was first identified (Adams and Brown, 1980). Further research found that the suppression of M-current is due to the activation of Gq, which is coupled with mAChR (Brown et al., 1989; Haley et al., 1998; Pfaffinger, 1988). Other types of receptors coupled to Gq, such as mGluR1 and mGluR5 metabotropic glutamate receptors, histamine H1, and several peptide receptors, can also inhibit the M-current (Brown and Passmore, 2009; Lee et al., 2010; Marrion, 1997).

The current mediated by KCNQ channels is characterized by slowly activating and non-inactivating properties (Brown and Passmore, 2009). The main functions of KCNQ channels in the CNS include regulation of AP initiation, propagation, and control of repetitive firing. KCNQ channels are essential in regulating the intrinsic excitability and gamma oscillation in neurons (Leao et al., 2009; Yue and Yaari, 2006). Additionally, KCNQ is expressed in the calyceal terminal. This channel is the major K^+ channels responsible for setting the resting properties of the calyx. Modulation of the

channel controls resting potential, resting conductance, subthreshold electrical activity, and neurotransmitter release probability of the calyx of Held (Huang and Trussell, 2011).

Mutations in all five genes of the KCNQ family (KCNQ1-5) encoding the Kv7.1-7.5 have been found to be associated with inherited diseases, including deafness, epilepsy, and cardiac arrhythmias. For example, a KCNQ1 mutation causes a heart disorder called Long QT Syndrome (Wang et al., 1996). Mutations in KCNQ2 (Biervert et al., 1998), KCNQ3 (Charlier et al., 1998), and KCNQ5 (Jentsch, 2000) cause neonatal convulsions, an inherited form of epilepsy, while mutations in KCNQ4 underlie congenital deafness (Kubisch et al., 1999). Due to the important function of KCNQ in the nervous system, many drug discoveries focus on KCNQ as a potential therapeutic target for disorders such as epilepsies, pain, and neurodegenerative and psychiatric disorders (Chen et al., 2017; Davoren et al., 2015; Gribkoff, 2003).

1.6 Aims of the study

To identify the sub-millisecond difference of binaural signals, the calyx-MNTB synapses are specialized for firing at very high frequency. Action potentials provide critical prerequisites: calcium influx to activate SK channels and the depolarization of membrane potential to open KCNQ channels. The generation of SK current and KCNQ current, in turn, shapes the action potential activities. We observed these K⁺ conductances in the calyx-MNTB synapse - SK channels in the postsynaptic MNTB neuron and KCNQ channels in the calyx of Held. Although the functions of SK channels and KCNQ channels in regulating neuronal excitability have been studied over

the years, their roles in this particular synapse are unclear. **The main objective of this thesis project was to address the functions of SK channels and KCNQ channels in the calyx-MNTB synapse.** One of the important purposes associated with the calyx-MNTB synapse having various types of K⁺ channels at both presynaptic and postsynaptic sites is the ability to transmit high-frequency signals reliably. For the reasons above, combined with the properties and features of SK channels and KCNQ channels, I aimed to test the hypothesis that both SK channels and KCNQ channels have essential roles in affecting the reliable high-frequency signal transmission in the calyx-MNTB synapse. In particular, my studies answer the following questions:

1. How are SK channels activated under physiological conditions?
2. Do SK channels open at RMP of MNTB neurons and what are the underlying mechanisms? How do they regulate the resting properties of MNTB neurons?
3. Are SK channels activated by APs? How do SK channels regulate the firing properties of MNTB neurons? Are they important for the reliable synaptic signaling at high frequency?
4. What are the features of high-frequency firing in the calyx of Held? Are KCNQ channels activated during high-frequency firing?
5. What are the functions of KCNQ channels during high-frequency firing? How do KCNQ channels regulate reliable high-frequency firing?

CHAPTER 2. MATERIALS AND METHODS

2.1 Slice preparation

The handling and care of animals were approved by the Institutional Animal Care and Use Committee of Tulane University and in compliance with U.S. Public Health Service guidelines. Brainstem slices containing the MNTB were prepared from P6-16 Wistar rats of either sex as previously described (Huang and Trussell, 2014). Briefly, 210 μm sections were cut in ice-cold, low- Ca^{2+} , low- Na^{+} saline using a vibratome (VT1200S, Leica), incubated at 32°C for 20–40 min in normal artificial cerebrospinal fluid (aCSF) and thereafter stored at room temperature before use. The solutions used in slicing, incubation, and recording are shown in Tables 2.1 and 2.2.

| Chemicals | Concentration (mM) |
|----------------------------------|---------------------------|
| Sucrose | 230 |
| Glucose | 25 |
| KCl | 2.5 |
| MgCl ₂ | 3 |
| CaCl ₂ | 0.1 |
| NaH ₂ PO ₄ | 1.25 |
| NaHCO ₃ | 25 |
| Ascorbic acid | 0.4 |
| <i>Myo</i> -inositol | 3 |
| Na-pyruvate | 2 |

Table 2.1 Saline for slicing.

Saline was bubbled with 5% CO₂/95% O₂.

| Chemicals | Concentration (mM) | Concentration (mM) |
|----------------------------------|--------------------|--------------------|
| CaCl ₂ | 2 | 1.2 |
| NaCl | 125 | 125 |
| Glucose | 25 | 25 |
| KCl | 2.5 | 2.5 |
| MgCl ₂ | 1 | 1.8 |
| NaH ₂ PO ₄ | 1.25 | 1.25 |
| NaHCO ₃ | 25 | 25 |
| Ascorbic acid | 0.4 | 0.4 |
| <i>Myo</i> -inositol | 3 | 3 |
| Na-pyruvate | 2 | 2 |

Table 2.2 The aCSF for incubation and recording.

ACSF was adjusted to pH 7.4 and bubbled with 5% CO₂/95% O₂.

2.2 Whole-cell recordings

Brain slices were transferred to a recording chamber and were continually perfused with aCSF (2–3 ml/min) warmed to ~32°C by an inline heater (Warner Instruments). Neurons were viewed using an Olympus BX51 microscope with infrared Dodt gradient contrast optics and a 40× water-immersion objective lens. Whole-cell current- and voltage-clamp recordings were made with a Multiclamp 700B amplifier (Molecular Devices). In some recordings as indicated, the EGTA concentration was increased to 1 or 10 mM by substituting for K-gluconate with equal osmolarity. Pipettes pulled from thick-walled borosilicate glass capillaries (WPI) had open tip resistances of 2–4 MΩ for postsynaptic recordings and 3–5 MΩ for presynaptic recording. Series resistances (4–15 MΩ) were compensated by 60%–80% (bandwidth 3 kHz). Pipette solution used for pre- and post-synaptic recording are shown in table 2.3.

To examine the SK activation under voltage-ramp and -step experiments, TTX (0.5 μM), margatoxin (10 nM), and CsCl (2 mM) were added to block the Na⁺, Kv1, and HCN channels, respectively, which enhanced space-clamp and provided stable recordings.

To isolate the transient SK currents, picrotoxin (50 μM), strychnine (1 μM), DNQX (20 μM), (R)-CPP (5 μM), and TTX (0.5 μM) were added to the recording solution to block the GABA, glycine, AMPA, and NMDA receptors, and voltage-gated Na⁺ channel-mediated current, respectively. CaCl₂ and MgCl₂ were adjusted to 2.0 mM and 1.0 mM, respectively.

EPSCs were evoked by using a bipolar electrode positioned to the midline. To record NMDA receptor-mediated EPSCs, strychnine (1 μM), picrotoxin (50 μM) and NBQX (20 μM) were added to the recording solution. Pipette solution used for AMPA

receptor-mediated EPSC recordings is shown in Table 2.4. Strychnine (1 μM), picrotoxin (50 μM) and (R)-CPP (5 μM) were added to the recording solution.

To isolate the K^+ currents in calyx, TTX (0.5 μM), CsCl (2 mM), CdCl_2 (100 μM) and XE991 (10 μM) were added to the recording solution to block the Na^+ , HCN, Ca^{2+} and KCNQ channels.

To examine the Na^+ current in response to AP-voltage command templates, CdCl_2 (100 μM), Tetraethylammonium chloride (TEA-Cl) (10 mM), 4-aminopyridine (2 mM), CsCl (2 mM) and XE991 (10 μM) were added to block the Ca^{2+} , K^+ , HCN and KCNQ channels. NaCl in the aCSF was replaced by equimolar TEA-Cl. The intracellular solution for recording Na^+ currents is shown in Table 2.5. The same intracellular solution was used for recording presynaptic Ca^{2+} current. 0.5 μM TTX replaced 100 μM CdCl_2 to block Na^+ channels in recording solution.

Signals were filtered at 4-10 kHz and sampled at 10-50 kHz. Liquid junction potentials were measured (13 mV for K-gluconate-based and 10 mV for Cs-methanesulfonate-based internal solutions) and adjusted appropriately. Resting membrane potential was determined in current-clamp with zero holding current. Membrane conductance was measured using current ramps (from -100 pA to $+100$ pA at a duration of 100 ms) under current-clamp mode.

| Chemicals | Concentration (mM) | |
|----------------------------------|---------------------------------|----------------------------------|
| | Presynaptic pipette solution | Postsynaptic Pipette solution |
| K-Gluconate | 135 | 110 |
| KCl | 10 | 20 |
| MgATP | 4 | 4 |
| Tris-GTP | 0.3 | 0.3 |
| Na ₂ -phosphocreatine | 7 | 3 |
| EGTA | 0.2 | 0.2 |
| HEPES | 10 | 10 |
| MgCl ₂ | --- | 1 |
| Tris-phosphocreatine | --- | 10 |

Table 2.3 Post- and Pre- synaptic pipette solutions.

pH for both pipette solutions was adjusted to 7.3 with KOH, 290 – 295 mOsm.

| Chemicals | Concentration (mM) |
|----------------------------------|--------------------|
| Cs-methanesulfonate | 130 |
| CsCl | 10 |
| HEPES | 10 |
| EGTA | 5 |
| Tris-GTP | 0.3 |
| Mg-ATP | 4 |
| Na ₂ -phosphocreatine | 5 |
| QX-314 | 2 |

Table 2.4 Pipette solution for AMPA receptor-mediated EPSC recordings.

pH for pipette solution was adjusted to 7.3 with CsOH, 290 – 295 mOsm.

| Chemicals | Concentration (mM) |
|----------------------------------|--------------------|
| Cs-methanesulfonate | 120 |
| TEA-Cl | 20 |
| HEPES | 10 |
| EGTA | 5 |
| Tris-GTP | 0.4 |
| Mg-ATP | 3 |
| Na ₂ -phosphocreatine | 5 |
| MgCl ₂ | 1 |

Table 2.5 Pipette solution for examining sodium current.

pH for pipette solution was adjusted to 7.3 with CsOH, 290 – 295 mOsm.

2.3 Drugs

A list of all drugs and reagents used as part of this study is shown in Table 2.6. Drugs were stored as aqueous stock solutions at -20°C and dissolved in aCSF immediately before experiments. Drug solutions were applied by bath perfusion or pressure ejection ('puff').

2.4 Analysis

Data were analyzed using Clampfit (Molecular Devices) and Igor (WaveMetrics). The spontaneous transient outward currents were sampled by template matching using a rise time of 10 ms and decay of 20 ms, threshold of $4\times$ noise SD, using Axograph X. The voltage threshold of SK activation was detected under voltage-ramp protocols. The detection threshold for activation of SK current was determined from 200 Hz-filtered traces by extrapolating a line fitted between -100 and -90 mV; the point of deviation from this line ($2\times$ noise SD, typically obvious by visual inspection for a range of several pA) was considered as the point of detectable activation of SK.

Presynaptic voltage-gated currents were leak subtracted in Clampex (Molecular Devices) by using the P/N protocol with the AP waveform templates. Statistical significance was established using paired t-tests unless otherwise indicated. Data are expressed as mean \pm S.E.M.

| Compound | Supplier |
|----------------------------------|----------|
| KCl | Sigma |
| MgCl ₂ | Sigma |
| CaCl ₂ | Sigma |
| NaH ₂ PO ₄ | Sigma |
| NaHCO ₃ | Sigma |
| NaCl | Sigma |
| Glucose | Sigma |
| Ascorbic acid | Sigma |
| <i>Myo</i> -inositol | Sigma |
| Na-pyruvate | Sigma |
| MgATP | Sigma |
| Tris-GTP | Sigma |
| Na ₂ -phosphocreatine | Sigma |
| EGTA | Sigma |
| HEPES | Sigma |
| Tris-phosphocreatine | Sigma |
| Cs-methanesulfonate | Sigma |
| K-gluconate | Sigma |
| XE991 | Alomone |
| Apamin | Alomone |
| 1-EBIO | Alomone |
| TTX | Abcam |
| (R)-CPP | Abcam |
| Flupirtine | Alomone |
| Picrotoxin | Tocris |
| Strychnine | Sigma |
| Cadmium | Sigma |
| Margatoxin | Alomone |
| TEA-Cl | Sigma |
| CsCl | Sigma |
| QX-314 | Alomone |
| Glutamate | Sigma |
| 4-aminopyridine | Sigma |

Table 2.6 Drugs and suppliers.

CHAPTER 3. SK CHANNELS REGULATE RESTING PROPERTIES AND SIGNALING RELIABILITY OF A DEVELOPING FAST SPIKING NEURON

3.1 Abstract

Reliable and precise signal transmission is essential in circuits of the auditory brainstem to encode timing with submillisecond accuracy. Globular bushy cells reliably and faithfully transfer spike signals to the principal neurons of the medial nucleus of the trapezoid body (MNTB) through the giant glutamatergic synapse, the calyx of Held. Thus, the MNTB works as a relay nucleus that preserves the temporal pattern of firing at high frequency. Using whole-cell patch-clamp recordings, we observed a K^+ conductance mediated by small-conductance calcium-activated potassium (SK) channels in the MNTB neurons from rats of either sex. SK channels were activated by intracellular Ca^{2+} sparks and mediated spontaneous transient outward currents in developing MNTB neurons. SK channels were also activated by Ca^{2+} influx through voltage-gated Ca^{2+} channels and synaptically activated NMDA receptors. Blocking SK channels with apamin depolarized the resting membrane potential, reduced resting conductance and affected the responsiveness of MNTB neurons to signal inputs. Moreover, SK channels were activated by action potentials and affected the spike afterhyperpolarization. Blocking SK channels disrupted the one-to-one signal transmission from presynaptic calyces to postsynaptic MNTB neurons and induced

extra postsynaptic action potentials in response to presynaptic firing. These data reveal that SK channels play crucial roles in regulating the resting properties and maintaining the reliable signal transmission of the MNTB neurons.

3.2 Results

3.2.1 A spontaneous transient outward current mediated by SK channels

Spontaneous transient outward currents (STOCs) were detected in rat MNTB neurons under whole-cell voltage-clamp recordings with a K-gluconate based internal solution (Fig. 3.1). At -65 mV, these transient outward currents had an average amplitude of 65.3 ± 1.0 pA, a 10-90% rise time of 8.8 ± 0.1 ms and decay time constant of 17.4 ± 0.2 ms ($n = 11$). The STOCs were resistant to Na^+ channel blocker TTX and blockers for ionotropic AMPA, NMDA, GABA and glycine receptors, and metabotropic glutamate, GABA_B , muscarinic acetylcholine and dopamine receptors (data not shown). Instead, 100 nM apamin, a peptide that specifically blocks small- SK channels (Adelman et al., 2012), completely suppressed the STOCs (Fig 3.1A and C; $p = 0.004$, $n = 8$), indicating the involvement of SK channels in mediating the STOCs. We also tested the effects of 1-EBIO, an SK channel opener that enhances calcium sensitivity of SK channels (Pedarzani et al., 2001; Mateos-Aparicio et al., 2014), on the STOCs. 1-EBIO (100 μM) increased the frequency from 0.54 ± 0.20 Hz to 1.20 ± 0.38 Hz ($p = 0.03$) and slowed the decay time constant from 14.7 ± 1.1 ms to 42.5 ± 1.3 ms (Fig. 3.1D-G; $p < 0.0001$, $n = 5$). Meanwhile the overall STOC amplitude was decreased from 62.9 ± 6.7 to 45.9 ± 4.3 pA (Fig. 3.1H, $p = 0.005$, $n = 5$). The amplitude

distributions of STOCs were typically well-fitted with a Gaussian function; 1-EBIO did not largely affect the amplitude of the existing STOCs but created an apparently new STOC group with smaller amplitude (Fig. 3.1I).

During early postnatal development, the pre- and postsynaptic components of the calyx of Held synapse undergo a variety of morphological and functional changes. We then measured STOCs of the MNTB from rats of different age (Fig. 3.2A). At P6, 40% (8/20) MNTB neurons showed apparent STOCs (Fig. 3.2B-C). After reaching the peaks at P10-11, both the amplitude and the frequency of the STOCs started to decline and, at P14, STOCs were detected in only 1 out of 19 cells, and no apparent STOC were detected in P16 cells (Fig. 3.2B-C).

SK channels are activated by increases in cytosolic Ca^{2+} . STOCs in smooth muscle cells and neurons are activated by Ca^{2+} sparks resulting from spontaneous Ca^{2+} release from internal Ca^{2+} stores (Nelson et al., 1995; Arima et al., 2001; Cui et al., 2004). We found that ryanodine, an opener of ryanodine receptor that depletes internal ryanodine-sensitive Ca^{2+} stores, completely blocked the STOCs of MNTB neurons (Fig. 3.3A-B; $p = 0.003$, $n = 6$), indicating that the STOCs are triggered by the Ca^{2+} sparks caused by the opening of ryanodine receptor located in the endoplasmic reticulum. To test whether SK channels are in close to their Ca^{2+} source, we next examined the effects of Ca^{2+} buffering on STOCs. When the MNTB neurons were broken into a pipette solution contained 1 mM EGTA (compared to 0.2 mM EGTA in the standard solution), both the frequency and the amplitude of the STOCs were gradually decreased (Fig. 3.3C-E; $p = 0.02$, $n = 8$). When the pipette EGTA was increased to 10 mM, the STOCs were fully eliminated (Fig. 3.3F-G; $p = 0.009$, $n = 4$). These results indicate that SK channels are loosely coupled with Ca^{2+} sparks (Neher, 1998; Jones and Stuart, 2013). Ryanodine receptors can be activated by calcium-

induced calcium release in neurons (Verkhatsky and Shmigol, 1996). We then tested whether Ca^{2+} influx through voltage-gated Ca^{2+} channels (VGCCs) is required for triggering STOCs. Bath-application of 100 μM cadmium, a non-selective voltage-gated calcium channel blocker, for 15 min, decreased the STOC frequency from 0.54 ± 0.15 Hz to 0.22 ± 0.07 Hz (Fig. 3.3H-I; $p = 0.04$, $n = 7$) and reduced the STOC amplitude from 55.9 ± 7.0 pA to 41.5 ± 7.7 pA (Fig. 3.3J; $p = 0.0007$, $n = 7$). Therefore, Ca^{2+} influx through VGCCs facilitates the STOC activity. STOCs were then recorded at different holding potentials to test their voltage-dependence. When the cells were clamped at -100 mV, which is close to the Nernst K^+ equilibrium potential (E_K) of -102 mV, no apparent STOCs were detected. Depolarizing the membrane potential gradually increased both the amplitude and the frequency of STOCs. At around -50 mV, both the amplitude and the frequency reached their peaks. When the holding potential was further depolarized, however, the STOCs started to decline and disappeared at -30 mV (Fig. 3.3K-M).

FIGURE 3.1

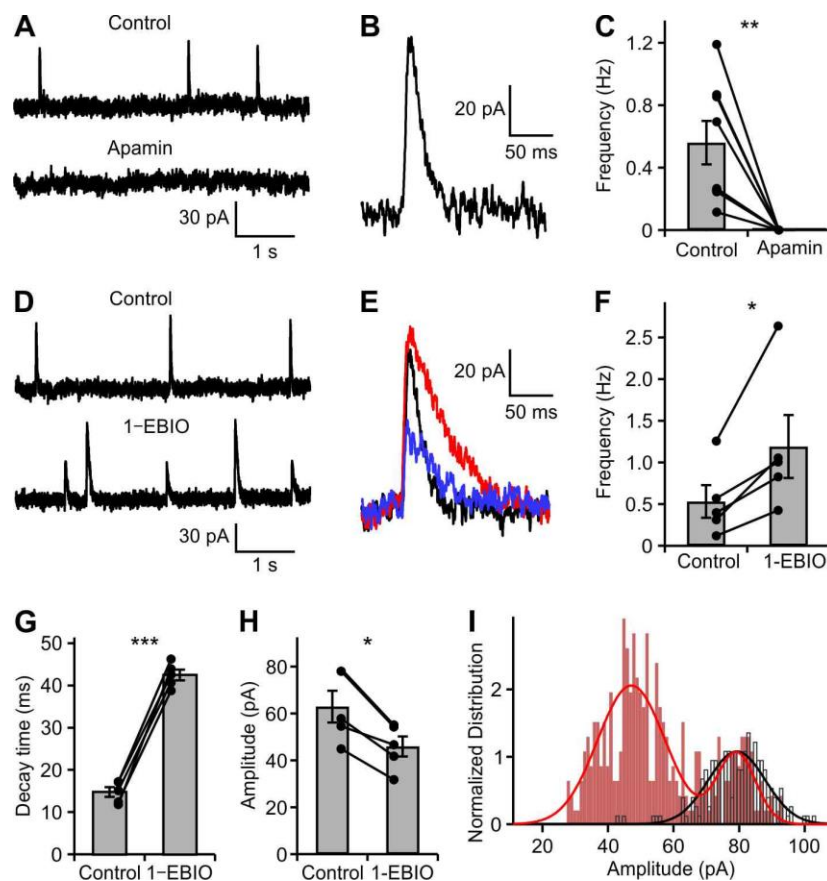


Figure 3. 1. SK channels mediated STOCs.

(A) STOC recordings in control and after bath application of 100 nM apamin. (B) A representative STOC event. (C) Summarize data of apamin effects on the STOC frequency. (D) STOC recordings in control and after bath application of 100 μM 1-EBIO. (E) Representative STOC events in control condition (black) and in the presence of 1-EBIO with different amplitudes (red and blue). (F-H) Summarize data of 1-EBIO effects on STOC frequency (F), decay time (G), and amplitude (H). (I) Amplitude distributions of STOCs recorded in the absence (black) and presence (red) of 1-EBIO, which were fit with one-component (black) and two-components (red) Gaussian

*functions, respectively. MNTB neurons were voltage-clamped at -65 mV. Recordings were made in the presence of 50 μ M picrotoxin, 1 μ M strychnine, 20 μ M DNQX, and 50 μ M APV to block the GABA, glycine, AMPA, and NMDA receptors, respectively. $*p < 0.05$; $**p < 0.01$; $***p < 0.001$; Paired Student *t*-test; Error bars are mean \pm SEM.*

FIGURE 3.2

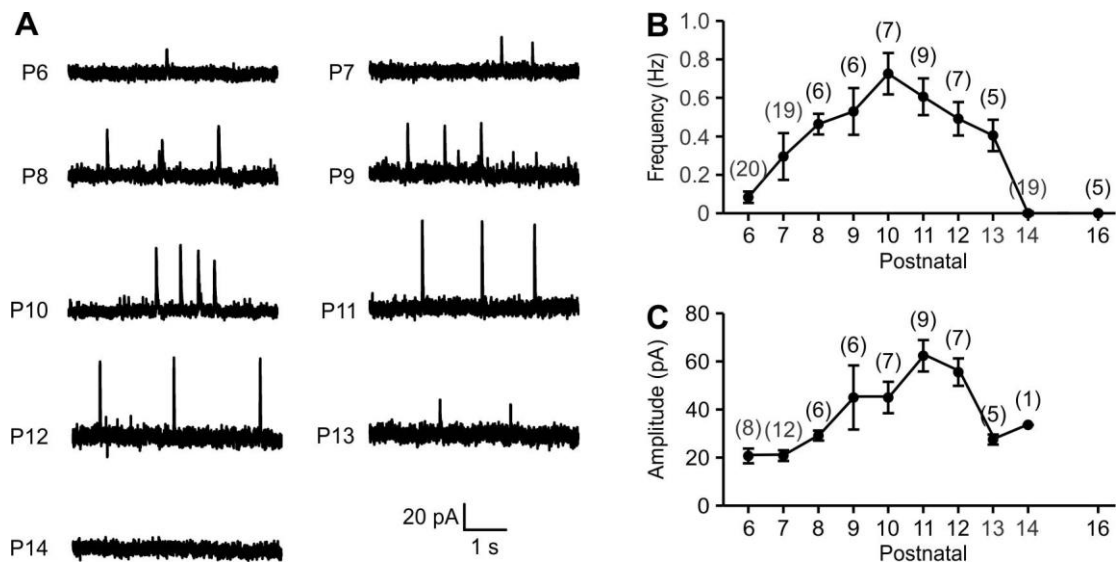


Figure 3. 2. Development change of STOCs.

A) Representative STOC recordings in rat MNTB neurons from P6 to P14. (B-C) Summary data of STOC frequency (B) and amplitude (C) change during development. Only cells with STOCs were included in the amplitude plot. For each postnatal day, the number of cells was indicated above the points.

FIGURE 3.3

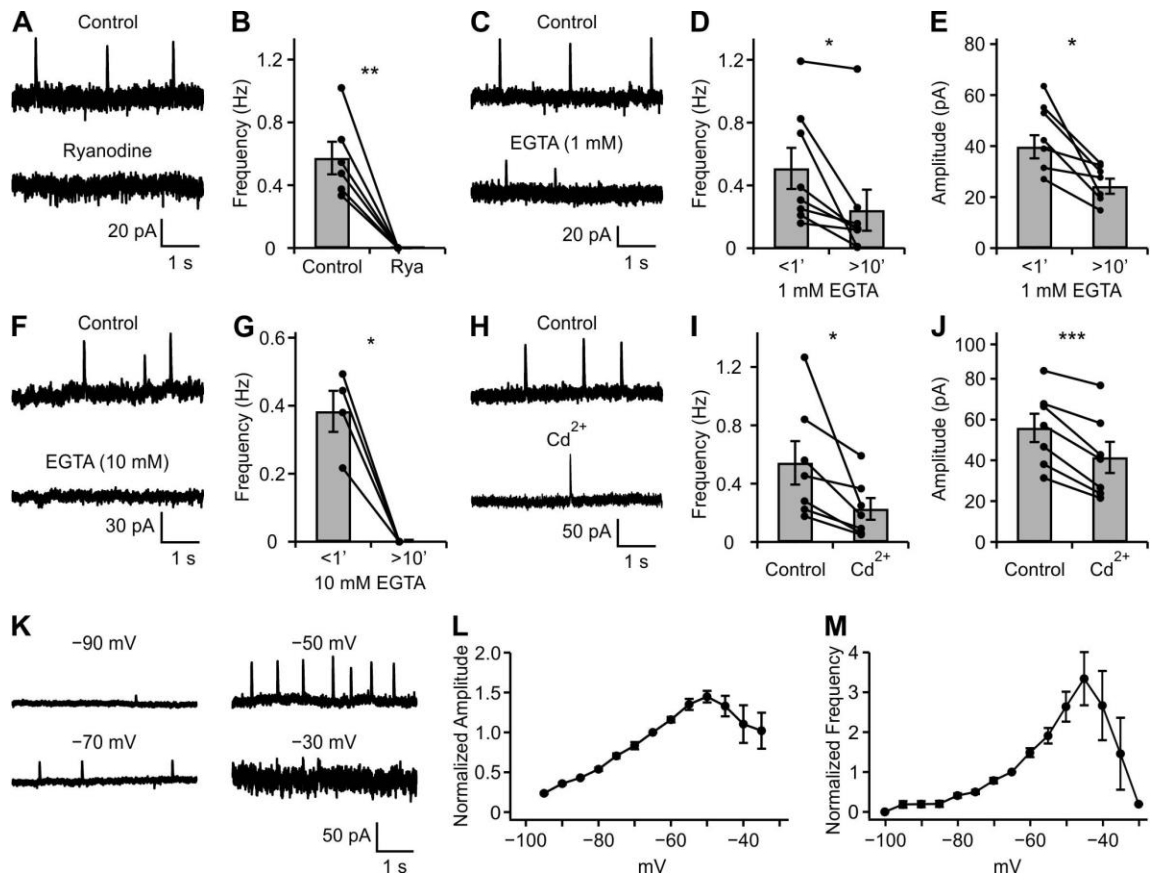


Figure 3.3. Calcium sparks activated the transient SK current.

(A) STOC recordings in control and after bath application of 20 μM ryanodine. (B) Ryanodine completely blocked the STOCs. (C) STOC recordings immediately (<1 min, control) and >10 min (EGTA) after break into a pipette solution containing 1 mM EGTA. (D-E) 1 mM EGTA decreased both the frequency and amplitude of the STOCs. (F) Same as panel C except the EGTA concentration was 10 mM. (G) The STOCs were eliminated by 10 mM EGTA. (H) STOC recordings under control conditions and after bath application of 200 μM CdCl₂. (I-J) STOC frequency and amplitude were decreased

by Cd^{2+} . (K) Representative STOC recordings at different holding potentials. (L-M) Normalized amplitude (L) and frequency (M) of STOCs at different holding potentials from -100mV to -30mV in 5 mV increment, normalized to the values at -65 mV . * $p < 0.05$; ** $p < 0.01$; *** $p < 0.001$; Paired Student t -test; Error bars are mean \pm SEM.

3.2.2 Activation of tonic SK Current

The decline of STOC amplitudes at depolarized voltages (> -50 mV) was unexpected, as depolarization increases the K^+ driving force. Indeed, the STOC amplitudes showed a linear relation with K^+ driving force ($E_M - E_K$) in different types of neurons (Merriam et al., 1999; Arima et al., 2001; Klement et al., 2010). We hypothesized that SK channels are tonically activated at depolarizations, and the STOCs are occluded by tonic SK activation. Voltage-step recordings were made in the presence of blockers of Na^+ , $Kv1$, and HCN channels (see Materials and Methods, which allowed us to clamp the membrane potential over a wider range of values to record the overall apamin-sensitive SK currents (Fig. 3.4A-B). By subtracting traces with 100 nM apamin from the control, a sustained current, in addition to STOCs, was detected (Fig. 3.4C; $n = 5$). This tonic current had an amplitude of 81.9 ± 21.0 pA at -40 mV. Thus, we concluded that SK channels are tonically activated when the MNTB neurons are depolarized.

SK channels do not desensitize, and the open probability of these channels solely depends on the cytosolic Ca^{2+} (Hirschberg et al., 1998), allowing us to examine SK currents using voltage-ramp protocols. A slow voltage ramp (5 mV/s) from -100 mV to -40 mV evoked an outward current with STOCs rising at depolarized voltages (Fig. 3.5A). This outward current was partially suppressed by bath application of 100 nM apamin. By subtracting the apamin trace from the control, a current-voltage relation of SK channels was determined (Fig. 3.5B). The tonic SK current had an amplitude of 90.9 ± 20.4 pA at -40 mV and the threshold for detection of current (see Materials and Methods) was remarkably negative (-85.5 ± 3.0 mV; $n = 6$). By contrast, 1-EBIO (100

μM) enhanced the outward current for 110.6 ± 20.6 pA at -40 mV (Fig. 3.5C; $n = 4$). Since the voltage-insensitive SK channels are not activated by voltage *per se* (Adelman et al., 2012), the activation of SK channels may reflect the Ca^{2+} elevation by the activation of VGCCs. Indeed, apamin did not affect the outward current evoked by the same voltage-ramp in the presence of 100 μM cadmium (Fig. 3.5D; $p = 0.87$, $n = 4$), indicating that the sustained SK current is activated by Ca^{2+} influx through VGCCs. The previous study showed that MNTB neurons express R-type, N-type, and P/Q-type, but not T-type, Ca^{2+} channels (Barnes-Davies et al., 2001), we then identified the VGCC subtypes that contribute to the SK activation. Low concentrations of Ni^{2+} (100 μM), specific for R- type and T-type channels (Wu et al., 1998; Kampa et al., 2006), shifted the activation threshold to -62.3 ± 0.9 mV (Fig. 3.5E-F; $n = 7$; $p < 0.001$, unpaired t-test). However, TTA-P2 (2 μM), a specific T-type blocker, did not affect the activation threshold (Fig. 3.5G-H; -80.3 ± 7.0 mV; $n = 5$; $p = 0.51$, unpaired t-test). These data indicate that calcium-permeable ion channels sensitive to Ni^{2+} and Cd^{2+} , likely R-type Ca^{2+} channels, control the tonic activation of SK channels at or around resting membrane potentials.

We next tested if ryanodine-sensitive Ca^{2+} stores are required for the tonic SK activation. In the present of 20 μM ryanodine, neither the threshold (-80.4 ± 6.6 mV; $n = 5$; $p = 0.50$, unpaired t-test) nor amplitude (122.1 ± 12.36 pA at -40 mV; $n = 5$; $p = 0.25$, unpaired t-test) of the tonic SK current is changed (Fig. 3.5I-J), suggesting that VGCCs, rather than calcium release from stores, is the Ca^{2+} sources to generate the tonic SK current.

FIGURE 3.4

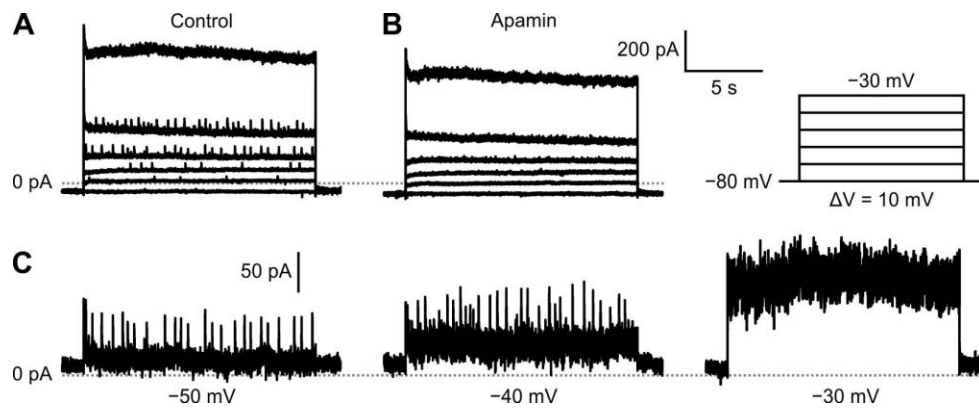


Figure 3. 4. Tonic SK current.

(A-B) Depolarizing voltage steps (15 s) from a holding potential of -80 mV to -30 mV in the increment of 10 mV evoked outward currents in control (A) and after bath application of 100 nM apamin (B). (C) Apamin-sensitive currents at different holding voltages obtained by subtracting the traces in panel B from that of A, showing the activation of tonic SK current along with the STOCs. Recordings were made in the presence of TTX (0.5 μ M), margatoxin (10 nM), CsCl (2 mM) to block the Na^+ , KVI and HCN channels, respectively.

FIGURE 3.5

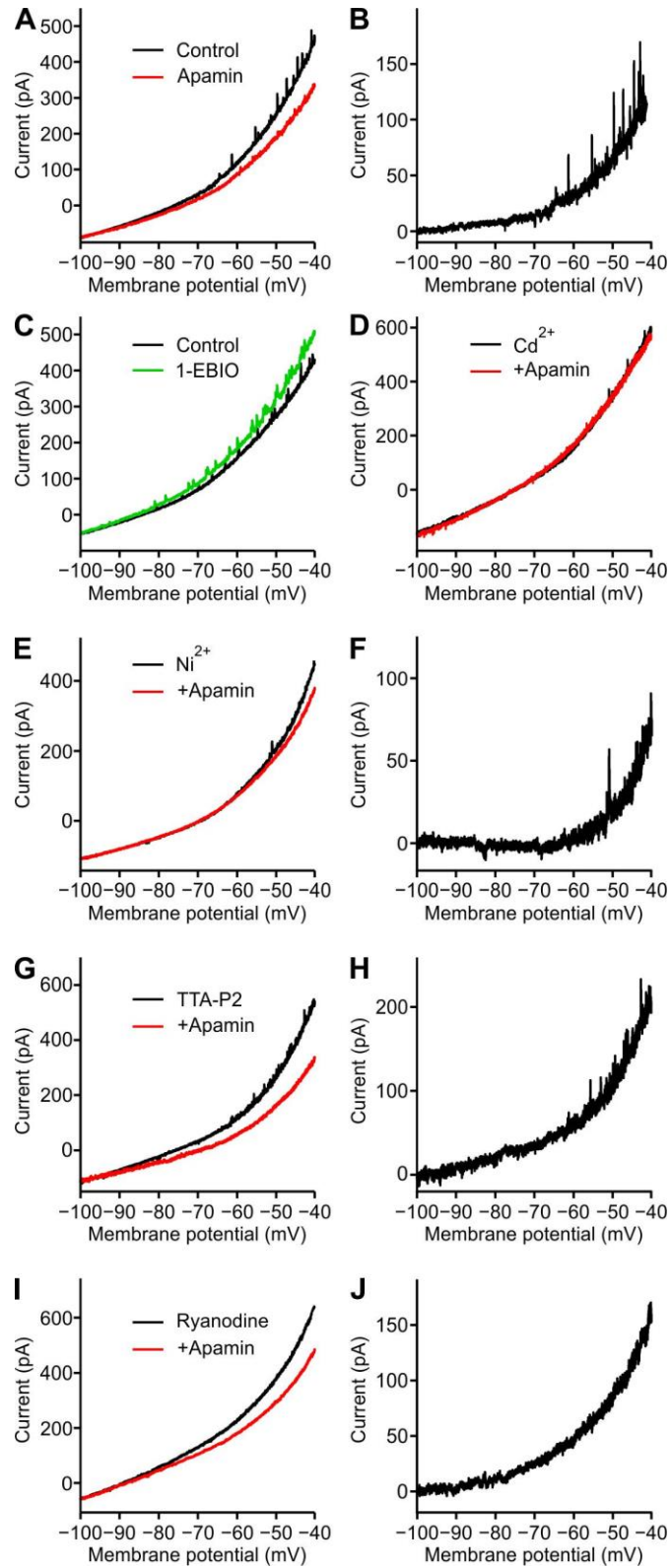


Figure 3. 5. Activation of SK current.

(A) A slow voltage ramp (5 mV/s) evoked an outward current (black) that was partially blocked by 100 nM apamin (red). (B) Apamin-sensitive current, obtained by subtracting the red trace from the black in A. Activation SK current was apparent at ~ -85 mV. (C) The voltage ramp-evoked outward current was potentiated by 100 μ M 1-EBIO. (D) In the presence of 100 μ M Cd^{2+} , application of apamin did not affect the outward current. (E) In the presence of 100 μ M Ni^{2+} , outward current recorded in control and after application of apamin. (F) The apamin-sensitive current obtained by subtracting the red trace from the black in E. (G-J) Similar recordings as E and F, except in the presence of 2 μ M TTA-P2 (G-H) or 20 μ M ryanodine (I-J). All recordings were made in the presence of TTX (0.5 μ M), margatoxin (10 nM), CsCl (2 mM).

3.2.3 SK channels contribute to resting membrane potential and conductance

The resting membrane potential of the MNTB neurons is typically -60 mV to -75 mV (Banks and Smith, 1992; Brew and Forsythe, 1995). Given that we detected the activation of SK current at -85 mV, one would expect that some channels should be open at the resting membrane potential and contribute to resting properties. Under current-clamp, we found indeed that puff application of 1 μ M apamin depolarized the resting membrane potential from -73.7 ± 0.6 mV to -72.1 ± 0.6 mV (Fig. 3.6A-B; $p = 0.0002$, $n = 6$). Meanwhile, the resting membrane conductance decreased from 5.4 ± 0.7 nS to 4.5 ± 0.6 nS (Fig. 3.6C; $p = 0.002$, $n = 6$).

By contrast, puff 1-EBIO (1 mM) hyperpolarized the membrane potential from -72.4 ± 0.7 mV to -73.8 ± 0.7 mV (Fig. 3.6D-E; $p = 0.001$, $n = 5$) and increased the resting membrane conductance from 5.9 ± 0.4 nS to 7.6 ± 0.5 nS (Fig. 3.6F; $p = 0.006$, $n = 5$). Accompanying membrane potential hyperpolarization, transient voltage hyperpolarizations were also observed, indicating the activation of STOCs. We concluded that SK channels are partially open at the resting potential and contribute to resting potential and resting conductance.

FIGURE 3.6

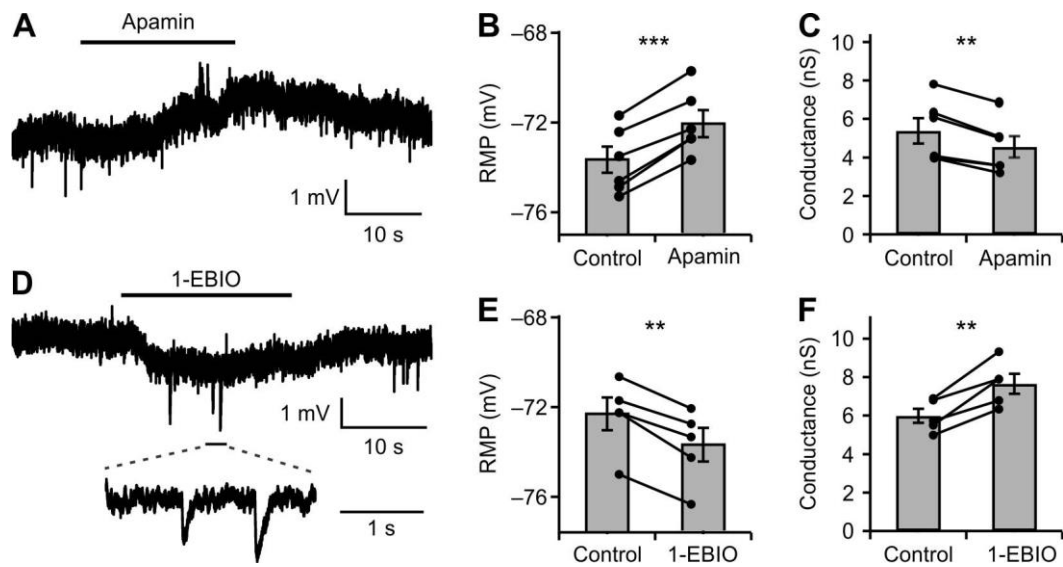


Figure 3. 6. Effects of SK channels on resting membrane properties of MNTB neurons.

(A-B) Puff application of 1 μ M apamin depolarized the resting potential by about -2 mV. (C) Bath application of 100 nM apamin decreased the resting conductance. (D-E) Puff application of 1 mM 1-EBIO hyperpolarized the resting potential. (F) Bath application of 100 μ M 1-EBIO increased resting conductance. **p < 0.01; ***p < 0.001; Paired Student t-test; Error bars are mean \pm SEM.

3.2.4 SK currents modulate signal responsiveness

Since SK channels are activated at resting membrane potential and contribute to resting conductance, we predicted that SK channels would modulate the response to stimulation. We injected MNTB neurons with current waveforms of different amplitudes to generate depolarizations (Fig. 3.7). Application of 100 nM apamin resulted in a 20% increase in the amplitude of the voltage response ($n = 5$; Fig. 3.7A-E). These results indicate that the effectiveness of subthreshold signaling is regulated by the activity of SK channels.

3.2.5 Activation of SK channels by NMDA receptors

SK channels are activated by Ca^{2+} through NMDA receptors in hippocampal and cortex neurons (Faber et al., 2005; Ngo-Anh et al., 2005; Faber, 2010). Electrical stimulation was used to evoke presynaptic glutamate release, and postsynaptic current was recorded. (R)-CPP was added into the recording solution to isolate the NMDA current. We found that apamin enhanced the synaptically activated postsynaptic NMDA current (Fig. 3.8A-B; $p = 0.004$; $n = 5$). By subtracting the apamin trace from the control, we obtained an NMDA receptor-activated SK current of 243.8 ± 56.4 pA ($n = 5$). However, the postsynaptic AMPA current was not affected when Cs^+ -based pipette solution contained 5 mM EGTA since they can eliminate the postsynaptic SK effect (Fig. 3.8C-D; $p = 0.34$, $n = 5$), indicating that SK channels did not affect presynaptic glutamate release. We also tested how SK channels modulate the excitatory postsynaptic potential (EPSP). 2 mM QX-314 was added into the pipette solution to

prevent spiking. Incubation of apamin (100 nM) increased the EPSP amplitude from 24.0 ± 3.8 mV to 27.6 ± 3.6 mV (Fig. 8E-F; $p = 0.009$, $n = 7$). Thus, Ca^{2+} influx through NMDA receptors activates SK channels, shunts the EPSP and regulates the synaptic efficacy.

FIGURE 3.7

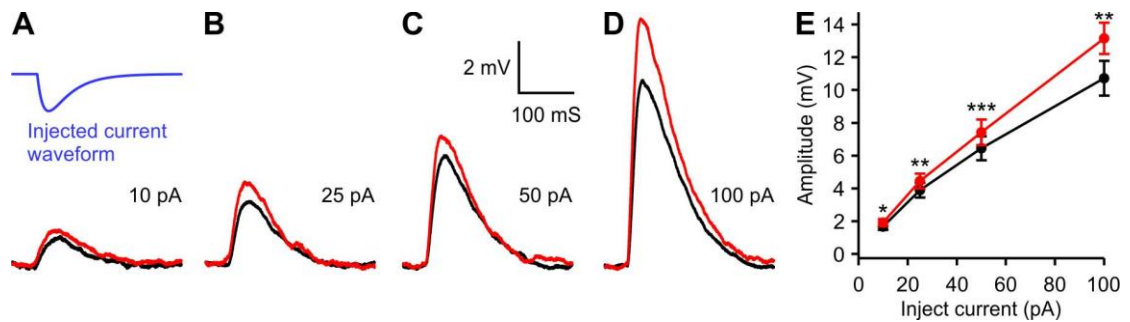


Figure 3. 7. Effects of SK channels on the responsiveness.

(A-D) Voltage responses to synaptic-like waveforms (rise time constant, 7.5 ms; decay time constant, 25 ms; A top trace) of different amplitudes injected into the MNTB neuron at control (black) or after bath application of 100 nM apamin (red). Voltage response traces were averages of 4–8 repeats. (E) Statistical data summarizing the apamin effects on the response amplitudes in A-D ($n = 5$). * $p < 0.05$; ** $p < 0.01$; *** $p < 0.001$; Paired Student t -test; Error bars are mean \pm SEM.

FIGURE 3.8

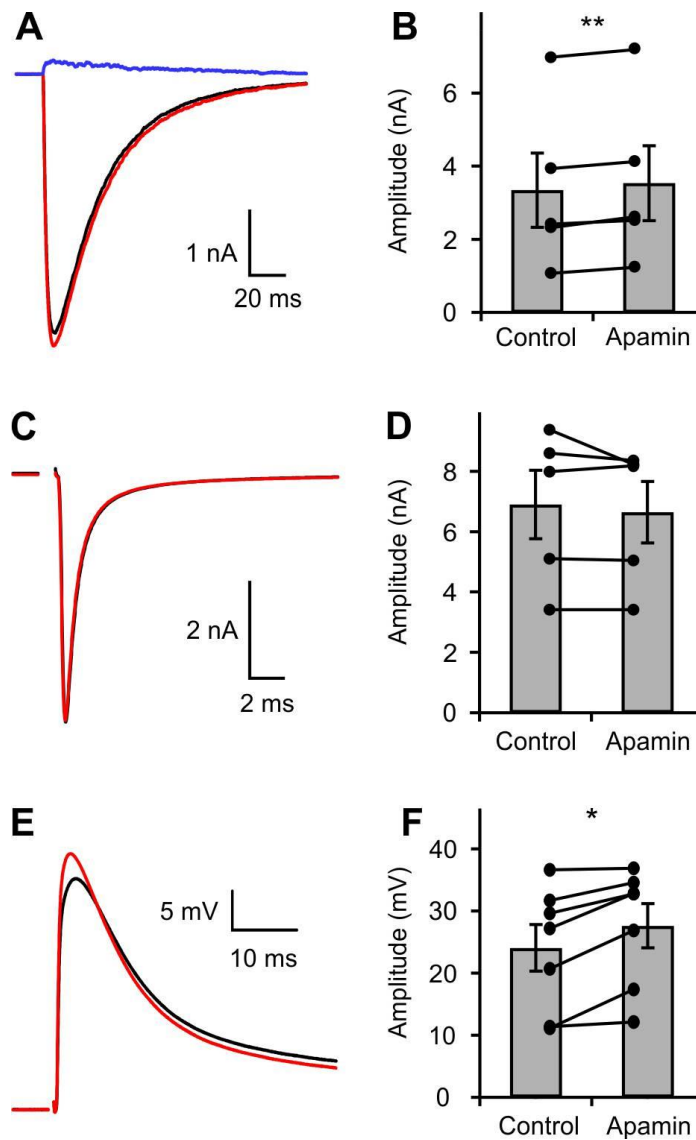


Figure 3. 8. Activation of SK channels by Ca²⁺ influx through NMDA receptors.

(A-B) Under voltage-clamp, extracellular Mg²⁺-free and K⁺-based internal solution, 100 nM apamin potentiated the NMDA receptor-mediated postsynaptic current. The blue trace in A represented NMDA-receptor-activated SK current obtained by

*subtracting the red trace (apamin) from the black (control). (C-D) With 5 mM EGTA, Cs⁺-based internal solution, the AMPA-receptor-mediated EPSC was not affected by apamin (100 nM). Black trace is AMPA-receptor-mediated EPSC in control condition, and red trace is recording after application of apamin. (E-F) Representative traces of EPSP before and after apamin (100 nM) application. 2 mM QX-314 were added into the pipette solution. Black trace is EPSP evoked in control condition and red trace is recording after application of apamin. * $p < 0.05$; ** $p < 0.01$; *** $p < 0.001$; Paired Student *t*-test; Error bars are mean \pm SEM.*

3.2.6 Activation of SK channels during action potential

In the presence of blockers for Na⁺, KV1, and HCN channel, a brief 1 ms voltage step from -80 mV to +10 mV was used to study the SK activation during action potential. This artificial spike triggered an inward Ca²⁺ current followed by an outward K⁺ current which is due to the activation of the high-threshold activating K⁺ channels - Kv3 channels. Bath application of 100 nM apamin significantly reduced the afterhyperpolarization current. Subtracting of the apamin trace from the control, an outward SK current was detected, which started during the depolarizing pulse, peaked at 8.4 ± 2.8 ms with an amplitude of 85.5 ± 19.2 pA, and decayed with a time constant of 9.1 ± 1.2 ms (Fig. 3.9A; n = 7).

Next, we examined how SK channels affect the waveform of synaptically-evoked action potentials. Presynaptic afferent fiber stimulation enabled us to record reliable and stable action potentials in MNTB neurons. Bath application of 100 nM apamin depolarized the afterpotential by 5.2 ± 0.6 mV (Fig. 3.9B; n = 6).

3.2.7 SK currents regulate reliability of signal transmission

Globular bushy cells fire action potentials up to hundreds of hertz during the sound. The high-frequency signals of globular bushy cells are faithfully transmitted to the postsynaptic MNTB neurons through the giant glutamatergic synapse, the calyx of Held, with few or no failures (Mc Laughlin et al., 2008; Lorteije et al., 2009). To test whether SK channel activity plays a crucial role in maintaining the faithful one-to-one signaling, we stimulated the presynaptic fiber and recorded the postsynaptic response.

At 100 Hz, each presynaptic stimulation evoked an action potential in MNTB neuron under control condition (Fig. 3.10A). Bath application with apamin disrupted the one-to-one reliability, and one presynaptic stimulation started to trigger two spikes in postsynaptic MNTB neurons after a few spikes (Fig. 3.10B), suggesting that the spike-activated SK current is critical in controlling MNTB excitability and prevent firing extra spikes.

A previous study showed that upon blocking KV1 channels with dendrotoxin, a single stimulus could evoke multiple presynaptic action potentials and multiple EPSCs in the MNTB neurons (Dodson et al., 2003), This led us to test whether apamin affects the presynaptic release during stimulation train. Bath application of apamin (100 nM) did not affect the one-to-one release, and each stimulus evoked a single EPSC during the whole stimulation train (Fig. 3.10C-D). Together with Figure 3.6, these results confirmed that apamin does not change the presynaptic firing properties or glutamate release.

FIGURE 3.9

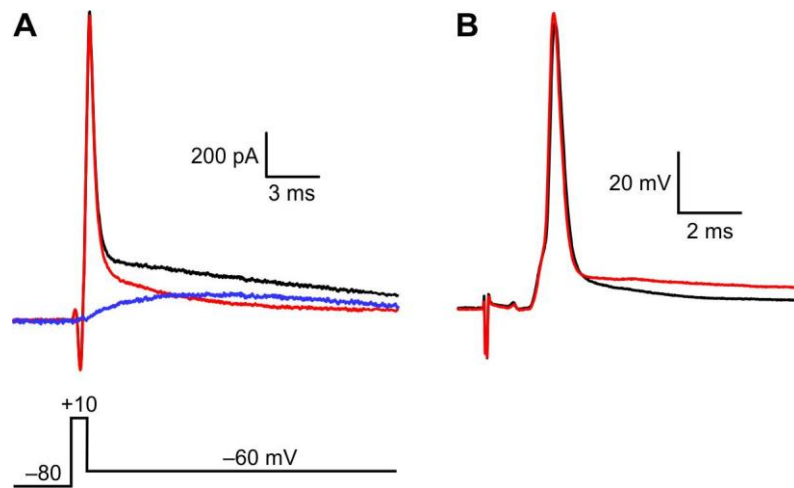


Figure 3. 9. Activation of SK channels during the action potential.

(A) A brief voltage-step to +10 mV was used to mimic the action potential evoked current. The current was recorded in control condition (black) and after bath application of 100 nM apamin (red). The blue trace represented the apamin-sensitive current. Recordings were made in the presence of 0.5 μ M TTX, 10 nM margatoxin, and 2 mM CsCl. (B) Presynaptic fiber stimulation-evoked action potentials recorded in control (black) and after bath application of 100 nM apamin (red). Recordings were made in the presence of strychnine (1 μ M), picrotoxin (50 μ M) to block the glycinergic and GABAergic synaptic transmission.

FIGURE 3.10

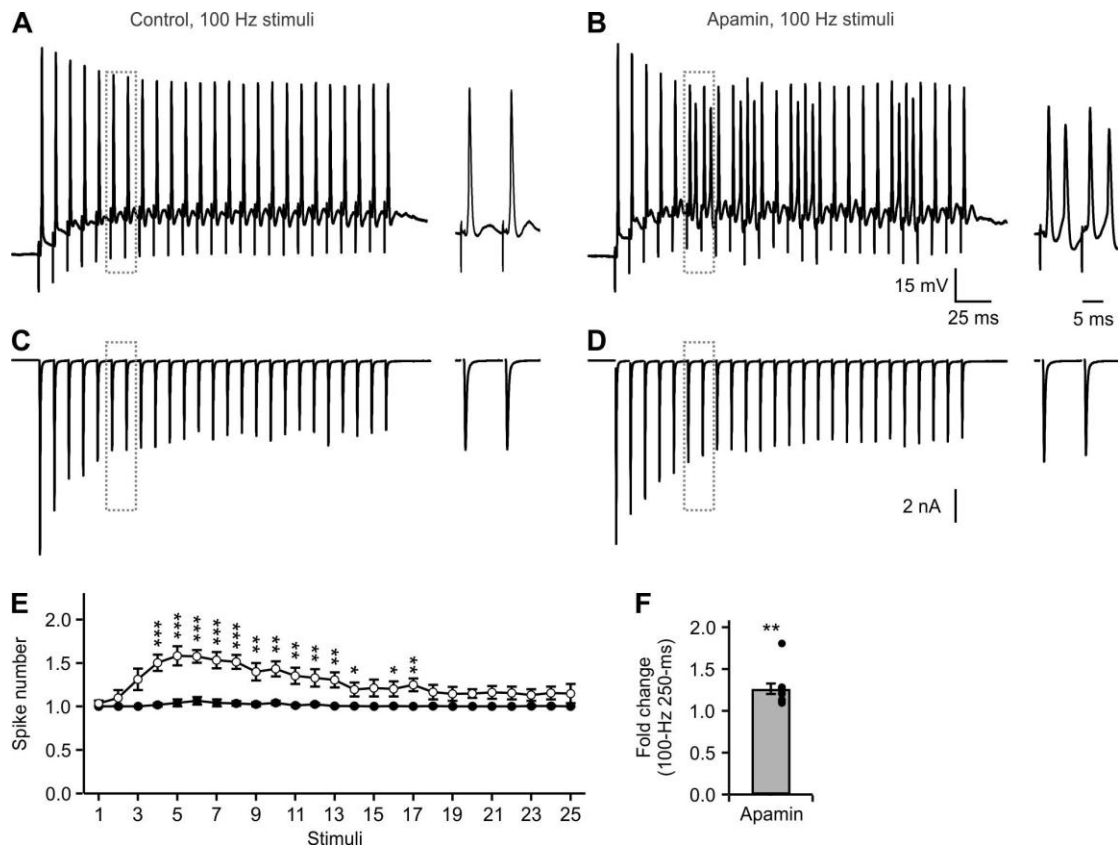


Figure 3. 10. SK channel activation was required for highly reliable signal transmission.

(A) Representative trace showing presynaptic 100 Hz stimulation generated a trains of action potentials in postsynaptic MNTB neurons. (B) Bath perfusion with apamin (100 nM), the stimulation generated extra action potentials in MNTB neurons. (C-D) EPSC recordings following 100 Hz stimulation in control (C) and with apamin (D). (E) Spike number counts after each stimulation before and after apamin application (n = 10). (F) Summary data that apamin increased the overall postsynaptic spiking in response to

*presynaptic stimulation. * $p < 0.05$; ** $p < 0.01$; *** $p < 0.001$; Paired Student t -test.*

Error bars are mean \pm SEM.

3.3 Discussion

In this study, we demonstrated a potassium conductance mediated by SK channels in rat MNTB neurons. SK channels are transiently activated by Ca^{2+} sparks and mediate the STOCs. SK channels can also be tonically activated by Ca^{2+} influx through VGCCs. Surprisingly, the tonic activation of SK channels controls the resting membrane potential and conductance, and thus the response of MNTB neurons to signal inputs. Moreover, SK channels are activated by Ca^{2+} influx through NMDA receptors and regulate the synaptic efficacy. Lastly, SK channels are activated by Ca^{2+} influx during action potentials and control the afterpotential and neuronal excitability. Blocking of SK channels disrupts the one-to-one signal transmission from the presynaptic calyces to the postsynaptic MNTB neurons. These data revealed that SK channels play important roles in controlling the resting properties and in ensuring the reliable and precise signal transmission in the MNTB neurons.

3.3.1 Activation of SK channels at MNTB neurons

While SK-channel subunits share the similar architecture and serpentine transmembrane topology of voltage-gated K^+ channels, these channels are voltage-independent K^+ channels activated solely by cytosolic Ca^{2+} (Blatz and Magleby, 1986; Xia et al., 1998). The elevations in cytosolic Ca^{2+} could result from several different sources, including Ca^{2+} influx through voltage-gated Ca^{2+} channels, Ca^{2+} influx via Ca^{2+} -permeable ligand-gated ion channels, Ca^{2+} released from

intracellular Ca^{2+} stores, and Ca^{2+} -induced Ca^{2+} release (Adelman et al., 2012). We found that SK channels in the MNTB neurons could be activated by all these Ca^{2+} sources.

SK channels were transiently activated by Ca^{2+} sparks and mediate STOCs (Figs. 3.1, 3). The nonselective VGCC blocker cadmium reduced the STOC amplitude and frequency, indicating that Ca^{2+} influx via Ca^{2+} channels facilitates STOC activity. However, blocking VGCCs failed to completely block STOCs, with 40% of STOCs remaining in the presence of cadmium. Ryanodine, however, fully abolished the STOCs at different voltages (Fig. 3.5I), suggesting that Ca^{2+} stores are essential and VGCCs indirectly modulate for STOCs. Thus, both spontaneous intracellular Ca^{2+} release and Ca^{2+} -induced Ca^{2+} release activate SK channels and mediate STOCs. The STOCs appear at \sim P6 and start to disappear at P14. The decline of STOCs after hearing onset may reflect the decline of SK channels, the decline of Ca^{2+} sparks, or the looser coupling between Ca^{2+} sparks and SK channels. Further experiment is necessary to clarify the mechanisms for development change of STOCs.

The amplitude distributions of STOCs were fitted with a Gaussian function (Fig. 3.1) while the SK channel opener 1-EBIO created an apparently new STOC group with a smaller amplitude, suggesting the heterogeneous Ca^{2+} sparks in MNTB neurons. At control conditions, only big Ca^{2+} sparks triggered STOCs while 1-EBIO increased the Ca^{2+} sensitivity of SK channels and small Ca^{2+} sparks were then able to activate SK channels and trigger STOCs. We found that lower-affinity Ca^{2+} chelator EGTA at 1 mM significantly decreased the frequency and the amplitude of the STOCs and 10 mM EGTA eliminated all STOCs (Fig. 3.3), indicating the loose coupling of Ca^{2+} sparks and SK channels at microdomains (Neher, 1998; Jones and Stuart, 2013). It is interesting that 1-EBIO did not affect the amplitude of the existing STOCs (Fig.

3.1*I*). A possible explanation is that at peak concentration, big Ca^{2+} sparks may saturate SK channels. Indeed, studies in hippocampal and cortical pyramidal neurons showed that Ca^{2+} sparks could extend to $>5 \mu\text{m}$ and reach peak concentration of $>5 \mu\text{m}$ (Ross, 2012).

3.3.2 SK channels and membrane properties

SK channels are extensively expressed in the nervous system and are gated by submicromolar concentrations of intracellular Ca^{2+} ions with a half-maximal activation concentration of $0.1\text{--}1 \mu\text{m}$ (Köhler et al., 1996; Joiner et al., 1997; Xia et al., 1998; Pedarzani et al., 2001). The activation of SK channels requires elevated levels of cytosolic Ca^{2+} , such as Ca^{2+} influx during firing action potentials. Under resting membrane potential, however, the cytosolic Ca^{2+} level is usually low, and SK channels are not active (Adelman et al., 2012). By contrast, our data in the MNTB neurons showed that SK channels were partially activated at resting membrane potentials. We detected a tonic SK current that starts to activate at $\sim -85 \text{ mV}$ (Fig. 3.5*B*), a voltage below the resting membrane potentials of -60 to -75 mV (Banks and Smith, 1992; Brew and Forsythe, 1995). Because SK channels are not activated by voltage per se (Adelman et al., 2012), the activation of SK channels should reflect the cytosolic Ca^{2+} elevation during the activation of VGCCs. Indeed, the tonic SK current was fully abolished by $100 \mu\text{m}$ cadmium (Fig. 3.5*D*). Consistent with that MNTB neurons express R-, N-, and P/Q-, but not T-type, Ca^{2+} channels (Barnes-Davies et al., 2001), we did not detect the contribution of T-type (Fig. 3.5*H*). Meanwhile $100 \mu\text{m}$ Ni^{2+} , a concentration believed to be specific for R- and T-type channels (Wu et al.,

1998; Kampa et al., 2006), shifted the activation threshold, suggesting that R-type Ca^{2+} channels are involved in the SK activation at voltages below -60 mV, although intermediate voltage-activated R-type channels are usually activated at more depolarized voltages. Alternatively, other calcium-permeable ion channels that sensitive to Cd^{2+} and Ni^{2+} may be responsible for the tonic activation of SK channels. At more depolarized voltages, the high-voltage gated N-type and P/Q-types would be involved.

The background conductance of MNTB neurons is mainly determined by two-pore potassium leak channels (Berntson and Walmsley, 2008). We found here that SK channels play a significant role in resting membrane properties of MNTB neurons, a result dependent entirely on the activation of SK channels at hyperpolarized voltages. Apamin depolarized the resting membrane potential and decreased the membrane conductance of MNTB neurons. Interestingly, in the calyx–MNTB synapse, totally different ion channels are involved in determining the resting membrane potential and conductance at the presynaptic and postsynaptic components. At the calyceal terminals, voltage-gated Na^+ , KCNQ and HCN channels contribute to the resting conductance (Cuttle et al., 2001; Huang and Trussell, 2008, 2011).

3.3.3 SK channels subserve auditory function

GBCs fire action potentials reliably and precisely synchronize to sound. For example, GBCs with the characteristic frequency of 700 Hz entrain to the sound and fire an action potential to every stimulus cycle with a phase-locking value of 0.99 (Joris et al., 1994). High-frequency signals of GBCs reliably transmit to the target MNTB

neuron through the calyx of Held synapse (von Gersdorff and Borst, 2002). Several cellular mechanisms have been established that are important for supporting neurotransmission at such high rates, including presynaptic ion channels that enable reliable presynaptic spike waveform and calcium influx; large readily releasable pool, many release sites, and low release probability that enhance the release reliability; as well as fast kinetics of postsynaptic AMPA-type glutamate receptors that allow fast and faithful transmission to the postsynaptic MNTB (Taschenberger and von Gersdorff, 2000; Taschenberger et al., 2002; Wu et al., 2009; Borst and Soria van Hoeve, 2012). Moreover, different voltage-gated K^+ channels are expressed on the presynaptic and postsynaptic components to control the neuronal excitability, determine spike shape, and enable high-frequency firing (Brew and Forsythe, 1995; Wang et al., 1998; Dodson et al., 2002; Ishikawa et al., 2003; Dodson and Forsythe, 2004; Huang and Trussell, 2011; Yang et al., 2014).

We found that SK channels are activated by Ca^{2+} through NMDA receptors in the MNTB neurons. The activation of SK channels partially offsets the EPSC and shunted the EPSP, thus regulating the synaptic efficacy. SK channels are activated by Ca^{2+} influx during a single or a burst of action potentials and mediate the afterhyperpolarization, thus controlling the intrinsic excitability in many neurons for setting the firing frequency and adaptation (Adelman et al., 2012). Here we measured the single action potential-triggered SK current in MNTB neurons. This 85 pA SK current peaked at a few milliseconds, lasted for tens of milliseconds, and mediated the medium afterhyperpolarization (Fig. 3.9). The calyx–MNTB synapse is a relay that transfers the presynaptic spike to the postsynaptic site and each presynaptic action potential evoked one action potential in the MNTB neurons. The evoked postsynaptic

action potentials displayed a distinct afterdepolarization. During 100 Hz firing, the afterdepolarization accumulated and substantially depolarized the membrane potential (Fig. 3.10). The relatively slow kinetics allow SK current summation during 100 Hz firing, thus counteracting the afterdepolarization and stabilizing the overall excitability. Interestingly, the activation of SK channels is required to maintain the reliable signaling at high-frequency. Bath application of apamin disrupted the one-to-one reliability, and each presynaptic stimulus started to trigger two postsynaptic spikes after a few spikes at 100 Hz stimulation (Fig. 3.10), while the reliability was not affected when the presynaptic stimulation is at 10 Hz (data not shown). This activity-dependent activation of the SK channel is different from that of voltage-gated K^+ channels, such as Kv1 channels. Blocking Kv1 channels changes the overall excitability, and each presynaptic action potential triggers multiple postsynaptic spikes no matter the firing frequency (Brew and Forsythe, 1995).

CHAPTER 4. KCNQ CHANNELS REGULATE FIRING PROPERTIES OF THE CALYX OF HELD

4.1 Abstract

Reliable and precise signal transmission is required in auditory brainstem circuits to localize the sound source. The medial nucleus of the trapezoid body (MNTB) works in the auditory circuits as an inverting relay nucleus that provides essential inhibitory signals for sound localization. To detect the sub-millisecond difference in the arrivals of binaural signals, the calyx of Held, the giant presynaptic terminal targeting to the MNTB neuron is able to faithfully follow, propagate and transmit high-frequency action potentials (APs). The waveform of the presynaptic AP shapes the presynaptic calcium transient and thus is crucial in determining timing and strength of synaptic transmission. During moderate- to high-frequency trains, the presynaptic APs of several central synapses such as mossy fiber boutons are altered, and the half-width of APs is substantially increased. However, the calyx of Held shows a minor AP broadening at frequencies up to hundreds of hertz. Using whole-cell patch-clamp recordings, we examined the functions of KCNQ channels in regulating the firing properties of the presynaptic terminal. We previously found that KCNQ channels localize in the calyceal terminal. Here we demonstrated that KCNQ channels were activated during depolarizations and high-frequency AP activity. KCNQ channels were required for the calyx to control the terminal excitability and maintain the normal presynaptic AP waveform at high-frequency firing. Blocking KCNQ channels with XE991 increased

presynaptic excitability, reduced the AP height, and broadened the AP half-width during high-frequency stimulation. It was further shown that blocking KCNQ channels led to cumulative inactivation of presynaptic Na⁺ channels and low-voltage-activated Kv1 potassium channels, and thereby indirectly affected the AP waveform. Application of low doses of TTX and margatoxin to partially block Na⁺ and Kv1 channels mimicked the AP waveform change during high-frequency firing. Constant AP waveform during high-frequency activity ensured that the calyx reliably triggers calcium influx. These data suggest that KCNQ channels play key roles in maintaining the presynaptic AP waveform during high-frequency firing, which further facilitates reliable high-frequency signal transmission by stabilizing the calcium inflow.

4.2 Results

4.2.1 KCNQ channels regulate the terminal excitability

KCNQ channels are widely distributed in the subcellular components of the neuron including soma, dendrite, and axon (Cooper et al., 2000a; Greene and Hoshi, 2016; Hu et al., 2007). Its roles in regulating excitability in soma and dendrite, but not the presynaptic terminal, are well described (Hu et al., 2007). Previous work from our lab has identified the expression of KCNQ channels in the calyx of held. (Huang and Trussell, 2011). To examine the contribution of KCNQ channels to terminal excitability, we recorded in the current clamp mode and applied a series of 1-s depolarizing current steps in 50 pA increments to the calyx. Inhibition and activation of KCNQ conductance had a striking effect on presynaptic excitability. Typically,

calyces responded to current pulses by generating only a few action potentials, regardless of the length of the pulse (Dodson et al., 2003; Ishikawa et al., 2003). As shown in Figure 4.1A-C&G, application of XE991, a KCNQ channel blocker, caused calyces to fire continuously at high rates for the duration of the stimulus. On average, XE991 increased the number of action potentials over 1 second from 5.0 ± 1.7 to 60.0 ± 15.7 ($p < 0.05$, $n=6$ calyces) for 50-pA current injection; from 15.2 ± 9.1 to 112.5 ± 18.3 ($p < 0.01$) for 100-pA current injection; from 21.3 ± 5.3 to 121.8 ± 24.6 ($p < 0.01$) for 150-pA current injection; and from 27.8 ± 8.4 to 135.8 ± 25.0 ($p < 0.01$) for 200-pA current injection. The KCNQ channels activator, flupirtine (Fig. 4.1D-F&H) decreased spike number from 4.3 ± 1.0 to 0.0 ± 0.0 ($p < 0.05$, $n = 4$ calyces) for 50 pA current injection; from 10.5 ± 2.1 to 0.5 ± 0.3 ($p < 0.05$) for 100 pA current injection; from 17.0 ± 3.7 to 1.0 ± 0.0 ($p < 0.05$) for 150 pA current injection, and from 21.5 ± 4.6 to 1.5 ± 0.3 ($p < 0.05$) for 200 pA current injection. Thus, changes in KCNQ current affected responses to both weak and strong stimuli. It is important to note that KCNQ channels in the calyx of Held have a relative hyperpolarizing activation threshold that is below the resting membrane potential (RMP) of the calyx. Accordingly, KCNQ channels contribute to set the resting properties of the calyx of Held (Huang and Trussell, 2011). Application of either drug caused a shift in resting potential. For these recordings, we injected bias currents to restore the membrane potential and repeated the pulse protocol. Values provided above were measured after restoring membrane potential. Together, they show that excitability of the terminal is dependent not only on the fast-gating channels that underlie the action potential, but also slow conductances like KCNQ that are active at or close to rest.

FIGURE 4.1

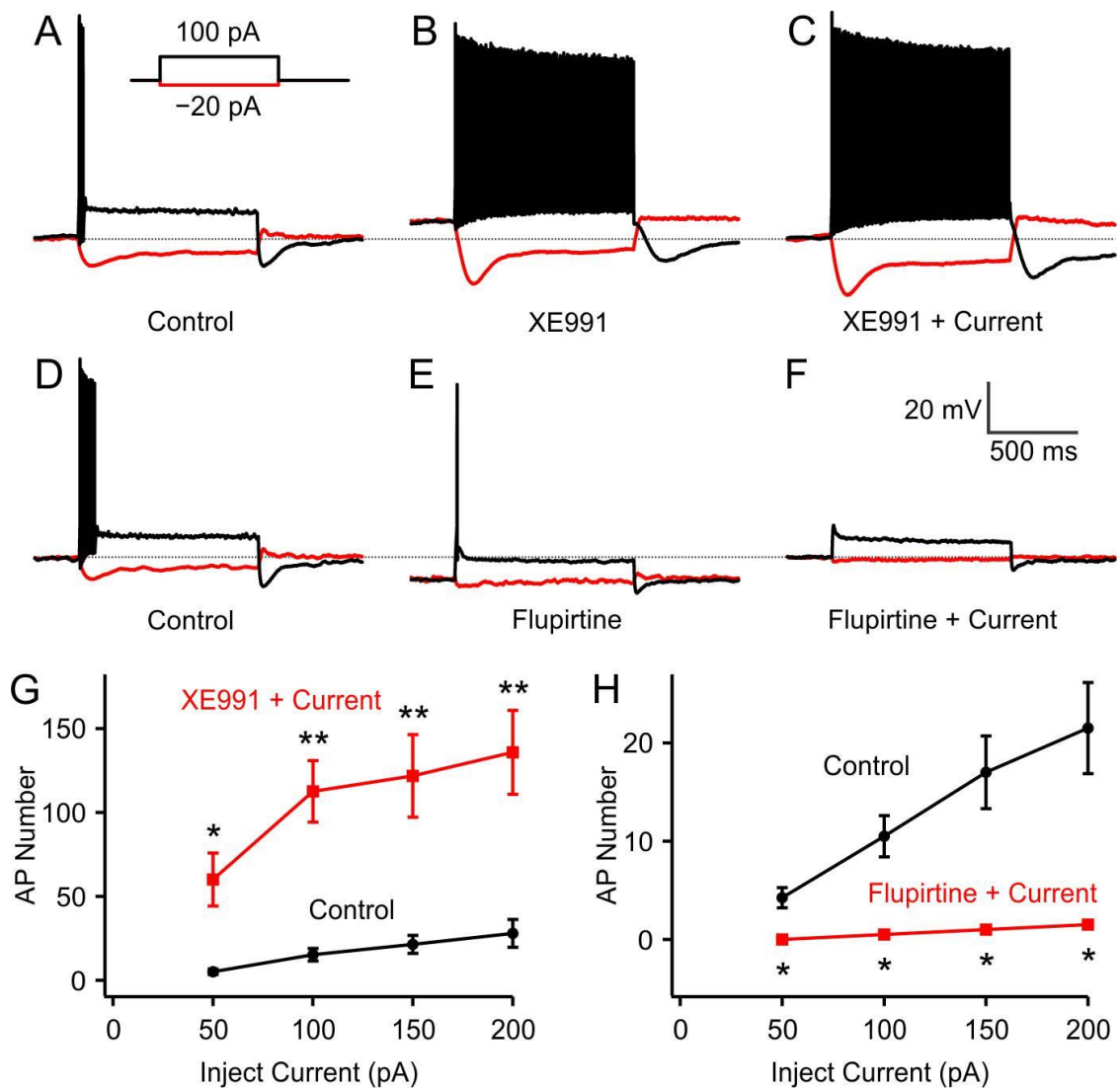


Figure 4. 1. KCNQ channels regulate the excitability of calyx of Held.

(A-C) APs elicited by 1-s, -20 pA (red) and 100 pA (black) current steps before (A) and after (B) bath application of 10 μ M XE991 to block KCNQ channels. Blocking

*KCNQ also led to the depolarization of RMP. Bias currents were injected (C) to correct for the depolarization of RMP. (D-F) APs elicited by 1-s, -20 pA (red) and 100 pA (black) current steps before (D) and after (E) bath application of 10 μ M flupirtine to open KCNQ channels. Bias currents were injected (F) to correct for the hyperpolarization of RMP induced by the opening of KCNQ channels. (G-H) Mean number of APs elicited by 1-s-long depolarizing current steps to the values given on the x-axis before and after bath application of XE991 (G) and flupirtine (H) with bias currents injection. XE991 increased, while flupirtine decreased, the total number of APs elicited by the 1 s-long depolarizing current steps. ** $p < 0.005$; * $p < 0.05$, Student t-test. Error bars are mean \pm SEM.*

4.2.2 Lack of activity-dependent AP broadening in calyx of Held

To distinguish sub-millisecond differences in the timing of binaural signals, the calyx is featured to firing at high-frequency up to hundreds of hertz after hearing onset (Lorteije et al., 2009; Taschenberger and von Gersdorff, 2000; Trussell, 1999). High-frequency AP activity-induced AP broadening has been reported in many terminals including the hippocampal mossy fiber boutons (MFBs) and pituitary nerve terminals (Geiger and Jonas, 2000; Jackson et al., 1991). We therefore examined the change of AP waveform in the calyx of Held during high-frequency firing. For this purpose, we stimulated the afferent fiber at midline to fire trains of 400 spikes at various frequencies (10, 33, 100 and 333 Hz) and recorded the AP trains at the calyx.

Results are illustrated in Fig. 4.2. For four recordings at different frequencies, every hundredth AP in the trains was superimposed with the first AP (Fig. 4.2A). The calyx fired with a stable waveform during the high-frequency stimulation. The half-width and amplitude of APs were maintained with remarkable constancy throughout the AP trains particularly at 10, 33 and 100 Hz. The maximal broadening of half-width was $18.9\% \pm 7.5\%$, and the maximal decrease of amplitude was $4.7\% \pm 1.5\%$ for 10, 33, 100 Hz AP trains. As we increased the stimulation frequency up to 333 Hz, we observed a slight activity-dependent AP waveform change. The maximal decrease of AP amplitude at 333 Hz stimulation was $34.3\% \pm 3.9\%$, while the maximal half-width increase was $91.2\% \pm 24.1\%$ (Fig. 4.2B and C; $n = 5$). Thus, we conclude that calyx of Held has the capability to fire at high frequency with stable AP waveform and the magnitude of AP waveform change is dependent on stimulation frequency.

FIGURE 4.2

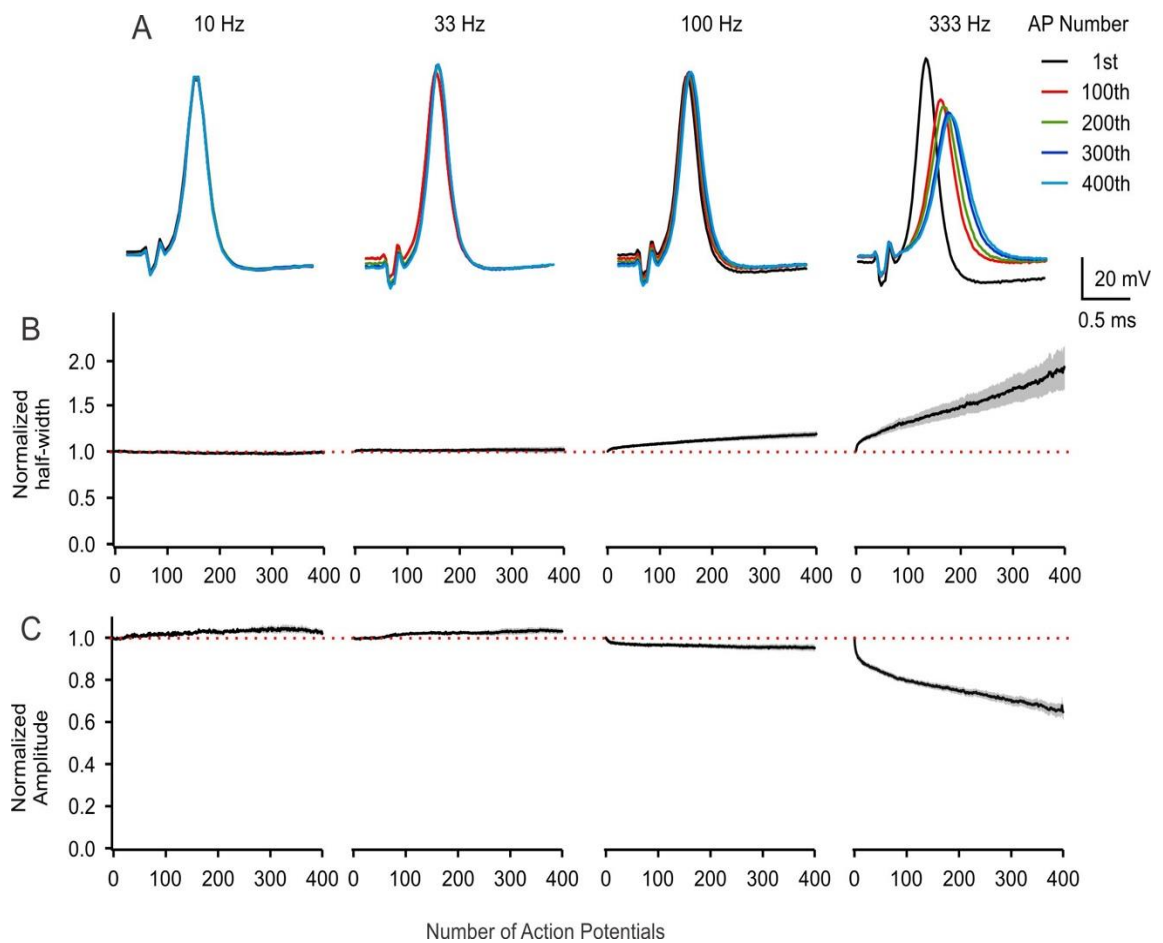


Figure 4. 2. Minimum AP waveform change during high-frequency AP activity in calyx of Held.

(A) Trains of APs evoked at the frequency of 10, 33, 100 and 333 Hz by afferent fiber stimulation. Every 100th AP is superimposed with the first AP in each recording at the

frequency indicated above. Plots of normalized half-width (B) and amplitude (C) of AP against the number of the AP within the trains for the frequency indicated. Data of each point is normalized to the value of the first AP in each train. Error bars are mean \pm SEM.

4.2.3 KCNQ contributes to maintaining AP waveform during high-frequency firing

We further explored the underlying mechanism in the calyx to prevent the AP waveform change during high-frequency activity. Here we defined the membrane potential between each spike in the AP trains as inter-spike potential (ISP). In general, ISP consists of the afterpotential following each spike in high-frequency firing. Change in afterpotential results in consecutive APs firing from different potentials. Interestingly, we observed that the ISP of AP trains at 333 Hz gradually hyperpolarized after a short-term depolarization during the first 50 spikes. In fact, this hyperpolarization of ISP during high-frequency activity in the calyx of Held is prevalent (Hee Kim et al., 2010a; Wang and Kaczmarek, 1998). However, little is known about the channels leading to the hyperpolarization of ISP. We postulate that the KCNQ channels take part in hyperpolarizing the ISP for several reasons. First, as a voltage-dependent potassium channel, opening of KCNQ channels could produce hyperpolarization of membrane potential. Second, with the slow-activating and non-inactivating properties, repetitive activation caused by high-frequency firing is able to produce a cumulative effect of KNCQ channels (Brown and Passmore, 2009; Huang and Trussell, 2011). KCNQ channels might have a minor impact on the first AP, but play an important role as the time of high-frequency firing is prolonged.

To test this hypothesis, we next examined the function of KCNQ channels during high-frequency firing using 400 APs elicited by afferent fiber stimulation at the frequency of 333 Hz. Fig. 4.3A-C illustrates the AP trains we recorded before and after application of 10 μ M XE991. Bias current was injected into the calyx to restore the

RMP to control level. After application of XE991, the hyperpolarization of ISP during high-frequency firing was eliminated. Bias current injections were unable to rescue fully but partially decelerated the hyperpolarization of ISP (Fig. 4.3F).

Accompanying the depolarization of ISP during high-frequency firing, we also observed a dramatic change of AP waveform. When the first and last APs in the spikes were contrasted, it is apparent that XE991 had a significantly greater impact on the waveform of the last rather than the first APs (Fig. 4.3D and E). The amplitude of the last AP was reduced, and the half-width was broadened after application of XE991. In contrast, the amplitude and half-width change of the first AP are comparable (Fig. 4.3G and H). When injected hyperpolarizing bias current to partially rescue the depolarization of ISP during the high-frequency firing, we observed that the shape change of the first AP was fully corrected, while the change of the last AP was partially corrected to control level. These results indicate the repetitive activation of KCNQ channels during high-frequency firing produce a gradual hyperpolarization of ISP, which is essential in maintaining AP waveform during high-frequency firing.

FIGURE 4.3

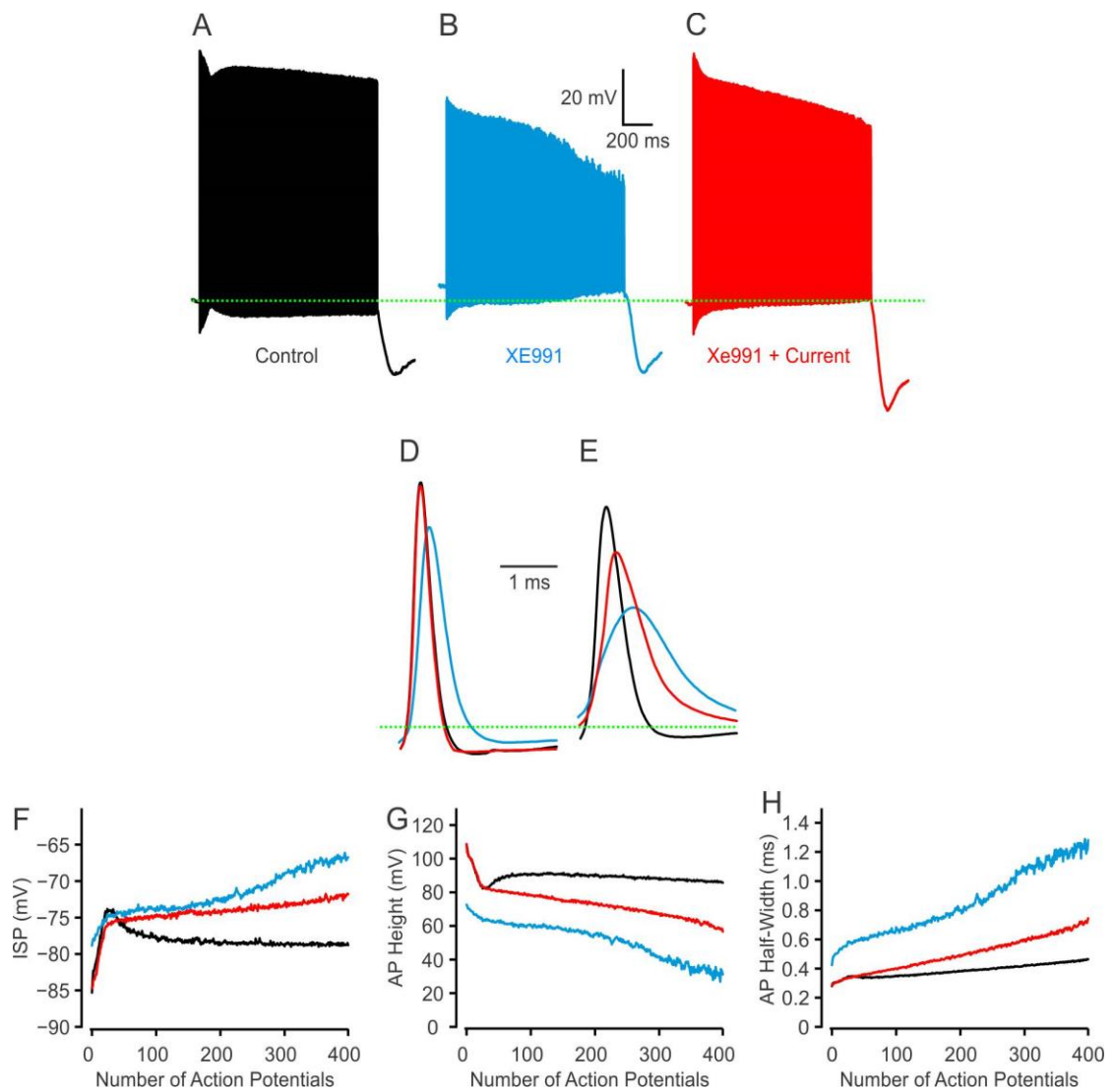


Figure 4. 3. KCNQ regulates the shape of APs during high-frequency AP activity in calyx of Held.

(A-C) Trains of APs elicited at the frequency of 333 Hz before (black) (A) and after (red) (B) bath application of 10 μ M XE991. Bias current was injected to restore the RMP to the value of control AP train (blue) (C). (D-E) The first (D) and last (400th) AP (E) in each train are superimposed at an expanded time scale. (F-H) Plots of ISP (F), height (G), and half-width (H) of APs against the number of the APs within the trains A, B and C.

4.2.4 KCNQ prevents the accumulative inactivation of Na⁺ and Kv1 channels in calyx during high-frequency firing

The afterpotential following the AP remarkably affects the recovery speed of Na⁺ and fast K⁺ channels. In consequence, it determines the total number of Na⁺ and fast K⁺ channels available for activation at the next AP (Brody and Yue, 2000; Bucher and Goillard, 2011; Sierksma and Borst, 2017a). Both Na⁺ and K⁺ channels are capable of shaping the AP waveform. However, their inactivations lead to differential results. For example, in MFBs, terminal Na⁺ conductance contributes to both the amplitude and half-width of AP (Bean, 2007; Engel et al., 2005). The cumulative inactivation of Kv1 channels, a low-voltage-activated K⁺ channel, is the primary factor causing the activity-dependent AP broadening (Dodson and Forsythe, 2004; Geiger and Jonas, 2000). Electrophysiological combined with immunocytochemical examinations have demonstrated that the calyx of Held and its affiliated axon express a high density of NaV and Kv1 channels, as well as the high-voltage-activated Kv3 channels (Huang and Trussell, 2008; Ishikawa et al., 2003; Leão et al., 2005; Nakamura and Takahashi, 2007; Puente et al., 2003; Sierksma and Borst, 2017a). The activation of KCNQ channels may affect the inactivation of Na⁺ and K⁺ channels to shape the waveform of AP during high-frequency firing via regulating the ISP. To investigate whether the existence of KCNQ channel influences the inactivation of Na⁺ and K⁺ during high-frequency firing, we attempted to directly record the change of I_{Na} and I_K by using naive 333 Hz stimulation AP trains as our voltage-clamp command templates. For better comparison of current change after running different AP trains, 10 ms-long depolarizing pulses were

added before and immediately after (3 ms behind the last AP) the control, XE991, and XE991+current AP trains (Fig. 4.4A and Fig. 4.5A).

We measured the currents evoked by the 10 ms depolarizing pulses before and after the AP trains with various channel blockers to isolate the current of NaV, Kv1, and Kv3, respectively (see Chapter 2: Materials and Methods). The remaining current was calculated by dividing the current evoked by the 1st depolarizing pulse with the 2nd one. We observed that the depressions of I_{Na} after running the XE991 and XE991+current command templates significantly increased compared with the control command templates. The remaining current evoked by the control AP trains templates is $65.8\% \pm 1.2\%$. It dramatically decreased to $26.6\% \pm 2.1\%$ and $25.8\% \pm 2.1\%$ in the XE991 and XE991+current AP trains templates, respectively (Fig. 4.4B and C; $n = 8$, control vs. XE991: $p < 0.001$; control vs. XE991 + current: $p < 0.001$). Isolated I_{kv1} with 1 mM TEA to block Kv3 channels obtained similar results. The remaining currents evoked by control, XE991, and XE991+current command templates were $64.1\% \pm 3.6\%$, $60.5\% \pm 2.6\%$, and $54.9\% \pm 2.7\%$ respectively (Fig. 4.5B – D; $n = 5$, control vs. XE991: $p = 0.04$; control vs. XE991 + current: $p < 0.001$). We also recorded the I_{kv3} using 10 nM margatoxin to block Kv1 channels and compared the changes. However, the remaining currents for I_{kv3} have no apparent difference for all 3 command templates (control: $50.1\% \pm 6.1\%$; XE991: $51.4\% \pm 6.1\%$; XE991 + current: $50.2\% \pm 6.1\%$). (Fig. 4.5E-G; $n = 7$, control vs. XE991: $p = 0.66$; control vs. XE991 + current: $p = 0.96$). These results suggest that KCNQ regulates the AP waveforms during high-frequency firing by preventing the cumulative inactivation of Na⁺ and Kv1 channels. Thus, the activation of KCNQ channels increases the availability of Na⁺ and Kv1 channels for generating upcoming APs.

FIGURE 4.4

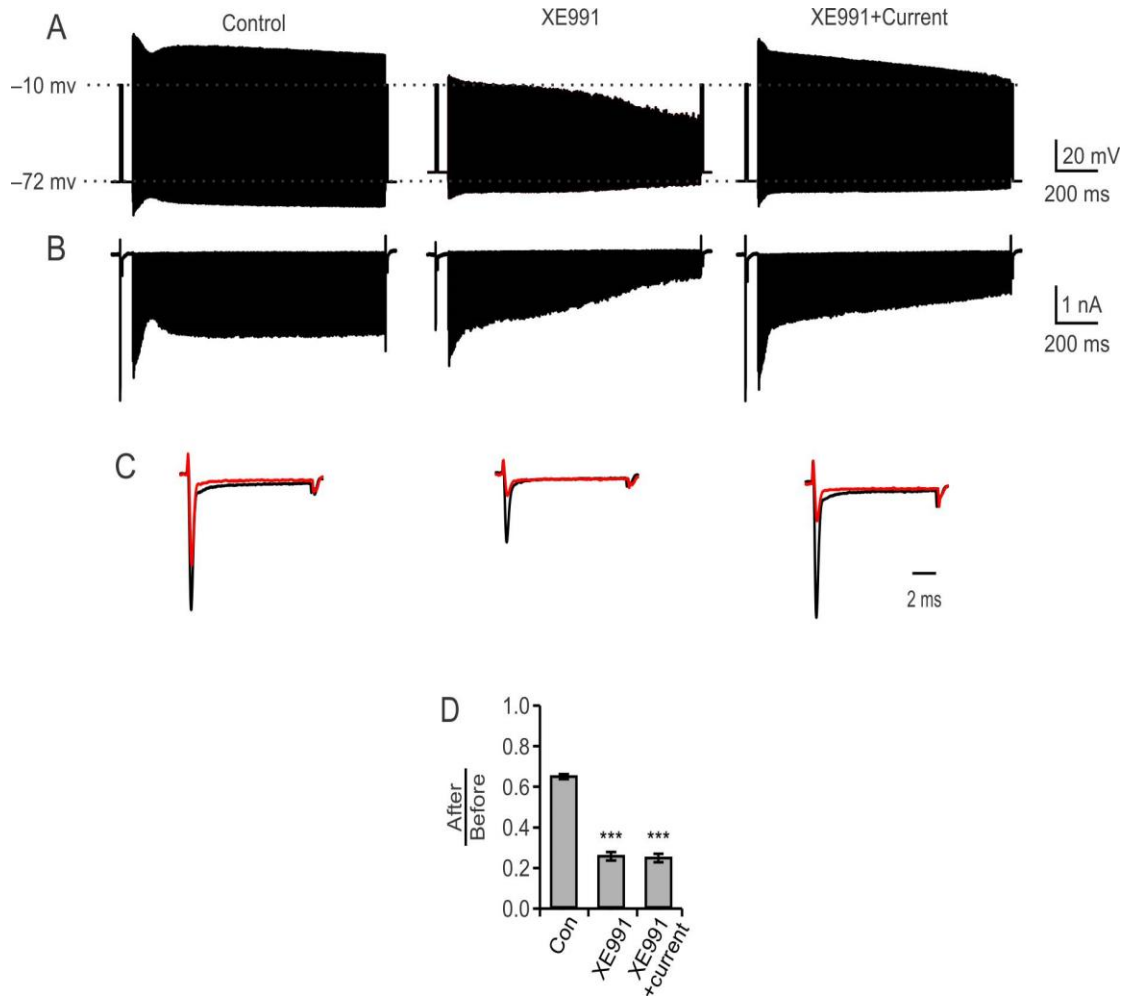


Figure 4. 4. KCNQ inhibits accumulative inactivation of Na⁺ channels at high-frequency firing.

(A) Command templates were created by adding 10 ms-long depolarizing pulses before and after naive control, XE991 and XE991 + current AP trains. To mimic the

*physiological condition, control and XE991 + current templates were clamped with initial holding potential at -72 mV; XE991 templates were clamped with initial holding potential at -66 mV. (B) Representative traces of I_{Na} evoked by the command templates after blockage of voltage-gated K^+ , Ca^{2+} , and HCN by a combination of external TEA + 4-AP + Cd^{2+} + Cs^+ + XE991 and internal TEA + Cs^+ . (C) I_{Na} evoked by the 1st (Black) and 2nd (Red) 10 ms-long depolarizing pulses were superimposed at an expanded time scale. (D) Summarizing data of the remaining I_{Na} for the control, XE991, and XE991 + current command templates. *** $p < 0.001$, student t -test. Error bars are mean \pm SEM.*

FIGURE 4.5

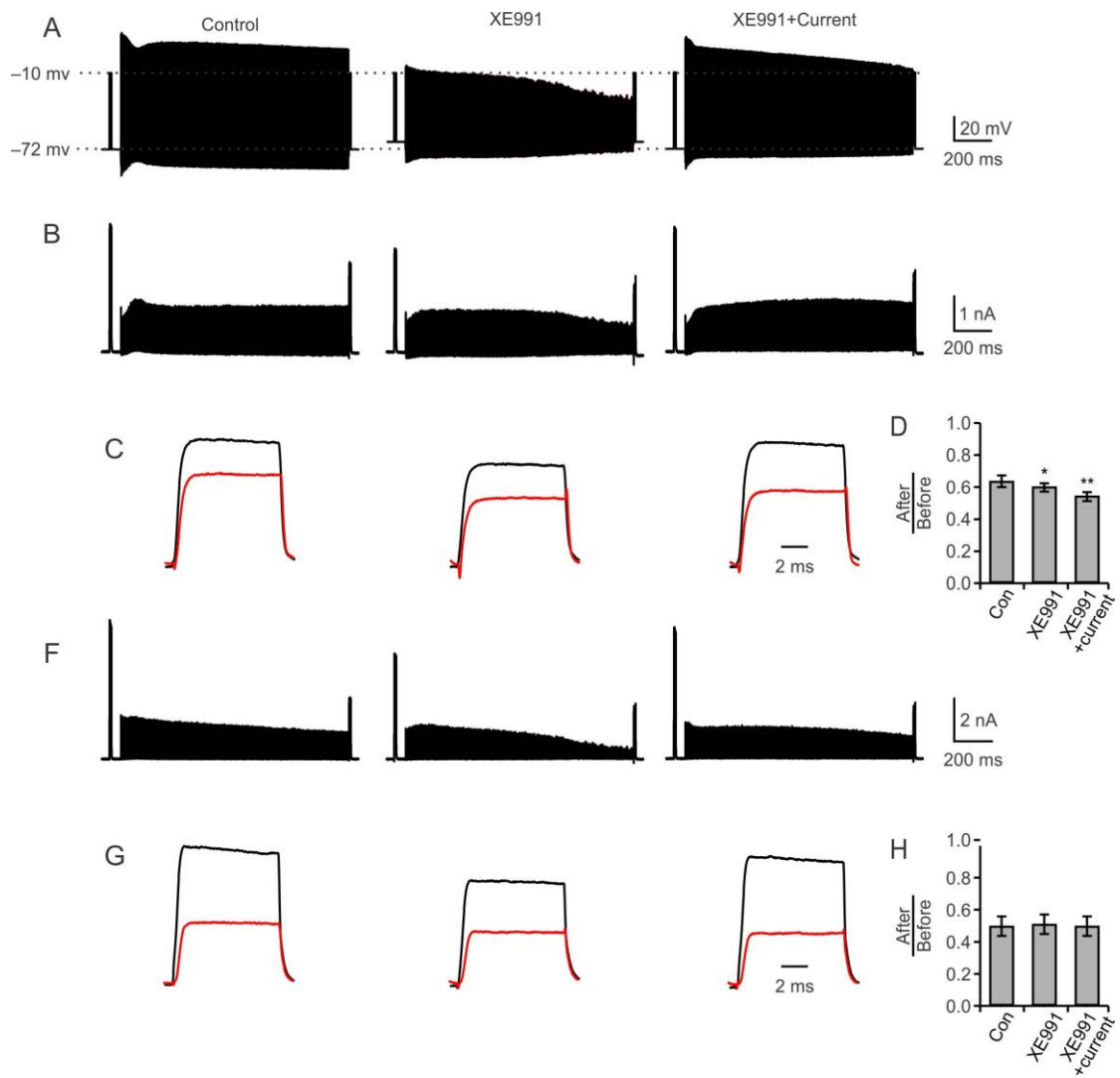


Figure 4. 5. KCNQ prevents the accumulative inactivation of Kv1, but not Kv3, for high-frequency firing.

(A) Command templates are the same as described in Fig.4.5A. (B) Representative traces of I_{Kv1} evoked by the command templates after blockage of voltage-gated Na^+ ,

Ca^{2+} , HCN, KCNQ, and Kv1 by a combination of external TTX + Ca^{2+} + Cs^+ + XE991 + 1mM TEA. (C) I_{Kv1} evoked by the 1st (Black) and 2nd (Red) 10 ms-long depolarizing pulses were superimposed at an expanded time scale. (D) Summarizing data of the remaining I_{Kv1} for the control, XE991, and XE991 + current command templates. (E) Representative traces of I_{Kv3} evoked by the command templates after blockage of voltage-gated Na^+ , Ca^{2+} , HCN, KCNQ, and Kv1 by a combination of external TTX + Ca^{2+} + Cs^+ + XE991 and margatoxin. (F) I_{Kv3} evoked by the 1st (Black) and 2nd (Red) 10 ms-long depolarizing pulses were superimposed at an expanded time scale. (G) Summarizing data of the remaining I_{Kv3} for the control, XE991 and XE991 + current command templates. ** $p < 0.005$; * $p < 0.05$, Student *t*-test. Error bars are mean \pm SEM.

4.2.5 KCNQ channels interact with Na⁺ and Kv1 channels to regulate the waveform of AP

To further test our hypothesis, we stimulated the afferent fiber to elicit single AP and first perfused 10 μ M XE991 to block KCNQ channels, and then partially blocked Na⁺ and Kv1 using TTX (10 nM) and margatoxin (50 pM) at low concentration. After XE991 perfusion, the half-width of AP increased slightly around $18.6\% \pm 5.8\%$ ($p < 0.05$), while the amplitude decreased about $14.7\% \pm 4.4\%$ ($p < 0.05$). The change of AP waveform after XE991 perfusion could be fully corrected by bias current injection, which closely repeated our observation of the waveform change of first AP in Fig. 4.3D. Further applied 50 pM margatoxin and 10 nM TTX gradually increased the AP half-width about $49.2\% \pm 7.8\%$ ($p < 0.005$) and declined the AP amplitude $40\% \pm 4.3\%$ ($p < 0.001$). Hyperpolarizing bias current failed to fully store the AP waveform change. Accordingly, we still observed an increase of AP half-width of $17.8\% \pm 4.4\%$ ($p < 0.05$) and decreased of AP amplitude of $21.3\% \pm 5.0\%$ ($p < 0.05$) (Fig. 4.6A and B; $n=5$). These results reinforce our interpretation that KCNQ channels interact with Na⁺ and Kv1 channels in the calyx to maintain the AP waveform during high-frequency firing.

FIGURE 4.5

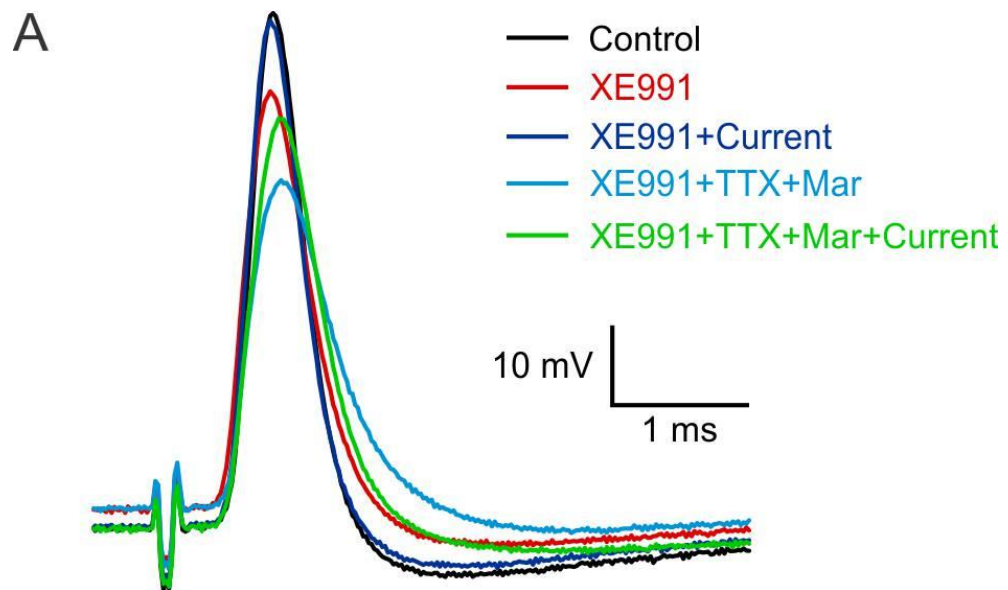


Figure 4. 5. KCNQ interacts with NaV and Kv1 channels to regulate the AP waveform.

(A) APs in the calyx were generated by afferent fiber stimulation. Bath application of 10 μ M XE991 induced the change of AP waveform, which could be restored by bias current injection. Gradually perfusion with 10 nM TTX and 50 pM margatoxin to partially block Na⁺ and Kv1 channels further increased the waveform change which could not be corrected by bias current injection. *** $p < 0.001$; ** $p < 0.005$; * $p < 0.05$, student *t*-test. Error bars are mean \pm SEM.

4.2.6 Function of KCNQ channels in regulating calcium response during high-frequency firing

Our results showed that KCNQ channels have important functions for calyceal terminals to stabilize the AP waveform during high-frequency firing. The shape of AP is the most critical determinant to affect the calcium charge transfer. The AP waveform affects both the amplitude of calcium current and the kinetics of activated VGCCs to mediate the total calcium influx (Wang et al., 2009; Yang, 2006a). To determine the effect of the KCNQ on regulating calcium current during high-frequency stimulation, we again employed the naive 333 Hz stimulation AP trains as our voltage-clamp command templates to evoke I_{Ca} (Fig. 4.7A). I_{Ca} was isolated and recorded using the same synapse under the condition that Na^+ , K^+ and HCN channels were blocked (Fig. 4.7B).

We measured the amplitude and the area integral of I_{Ca} evoked by each spike in the voltage-clamp command templates (Fig. 4.7E and F; $n = 5$). Fig. 4.7B provides examples of I_{Ca} evoked by the three voltage-clamp templates. The first and last I_{Ca} evoked in each AP templates were expanded and superimposed in Fig. 4.7C and D respectively. In all three recordings, the amplitude of I_{Ca} evoked by the command templates gradually decreased throughout the entire trains. The magnitude of amplitude changes of I_{Ca} induced by the first AP in each AP train (Control: -2.00 ± 0.14 nA; XE991: -1.2 ± 0.09 ; XE991+current: -1.87 ± 0.10) is smaller than the magnitudes in the last APs (Control: -1.75 ± 0.07 , XE991: -0.43 ± 0.06 , XE991+current: -1.43 ± 0.15). However, the change of the area integral differs the amplitude. We found that although the amplitude of I_{Ca} in the control and XE991+ current recordings slowly

decreased, the area integral gradually increased. The first I_{Ca} evoked by the first AP in the control and XE991 + current command templates have comparable area integral (control: -0.51 ± 0.05 nA·ms; XE991 + current: -0.50 ± 0.06 nA·ms, $p > 0.05$). As the AP waveform changed from the last AP in the control command template to the last AP in the XE991+ current command template, the area integral significantly increased (Control: -0.67 ± 0.06 nA·ms; XE991 + current: -0.86 ± 0.08 nA·ms, $p < 0.001$), which suggested an increase in the total Ca^{2+} charge transfer. Interestingly, the change of area integral evoked by the XE991 command template did not constantly increase or decrease. The XE991 command template initially produced a gradual elevation in area integrals, then the area integrals significantly declined below the level that had been evoked by the last response of the control command (last I_{Ca} evoked by XE991 command template: -0.37 ± 0.06 nA·ms, $p < 0.005$). The reduction in area integrals of I_{Ca} recorded by using the XE991 command template suggested that KCNQ channels are required to control the total Ca^{2+} charge transfer.

Together, these observations indicate that KCNQ channels during high-frequency firing have important effects on regulating the I_{Ca} . Hence, KCNQ channels help to maintain a stable AP waveform and ISP during high-frequency firing, which is important for stably evoking I_{Ca} .

FIGURE 4.7

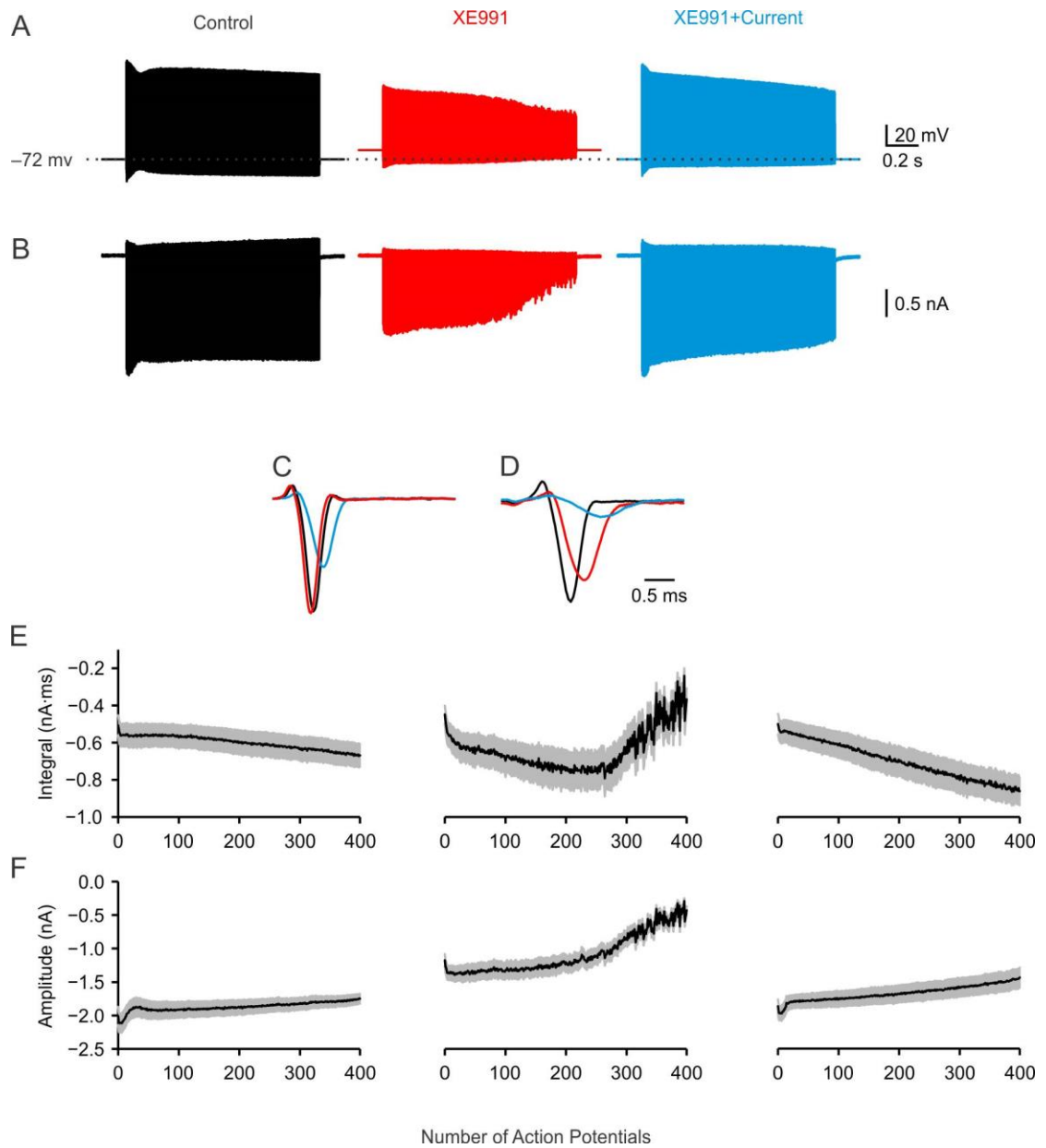


Figure 4. 6. Functions of KCNQ affect calcium currents during high-frequency AP activity.

(A) Naive control, XE991, and XE991 + current AP trains were used as voltage-clamp command templates (B) Representative traces of I_{Ca} evoked by three command templates with the same calyx. (C-D) First (C) and last (D) I_{Ca} in each recording are superimposed at an expanded time scale. (E-F) amplitudes (F) and integrals (E) of I_{Ca} were measured and plotted against the number of the APs within the three command templates.

4.3 Discussion

In this study, we demonstrated that KCNQ channels actively participate in regulating presynaptic excitability and AP activity in the calyx. KCNQ channels are activated during high-frequency AP activity and are required to maintain normal AP waveform of the calyceal terminal during high-frequency firing. KCNQ channels stabilize the AP waveform via controlling the accumulative inactivation of NaV and Kv1. Moreover, when firing at high-frequency, a stable AP waveform ensures that the calyx precisely generates calcium currents. This establishes a mechanism by which the calyx maintains the shape of APs during high-frequency firing to preserve reliable signal transmission.

4.3.1 KCNQ channels affect the presynaptic terminal excitability

KCNQ channels have a broad subcellular distribution that is directly related to their function. For example, in the CA1 pyramidal neuron, KCNQ channels regulate the neuronal excitability, and spike generation relies on the cluster in the perisomatic compartment instead of distal apical dendrites (Hu et al., 2007). Increasing evidence has indicated that KCNQ channels also have high-density distribution in the axon and presynaptic terminal (Caminos et al., 2007; Chung et al., 2006; Cooper et al., 2001). Previously published data performed with a combination of electrophysiological and immunohistochemistry approaches demonstrated that KCNQ channels are expressed in the calyx of Held (Huang and Trussell, 2011). Their function in regulating firing

properties in the presynaptic terminal has remained exclusive. By directly recording from the calyx of Held, we are able to test the importance of KCNQ channels affecting presynaptic excitability. Here we found that KCNQ channels indeed have a substantial function in reducing presynaptic terminal excitability. Either blocker XE991 or activator flupirtine of KCNQ channels significantly changed the AP generation induced by sustained depolarizing current injection (Fig. 4.1).

In the calyx, low-voltage-activated Kv1 channels were also reported to regulate synaptic terminal excitability (Nakamura and Takahashi, 2007). Blocking Kv1 with magatoxin induced a burst of spikes during sustained depolarization. It is not surprising that to ensure the fidelity of high-frequency signal transmission, the calyx incorporates various types of K⁺ channels to limit the excitability. Unlike the KCNQ channels that have more negative activation voltage, slow activation, and no inactivation kinetics, Kv1 channels have more positive activation voltage (around -40 mV), fast activation, and a small fraction of inactivation (Dodson et al., 2002; Ishikawa et al., 2003; Nakamura and Takahashi, 2007). The distinct properties of KCNQ channels and Kv1 channels indicate that they may have complementary physiological functions in regulating presynaptic excitability. Kv1 channels react more quickly while KCNQ channels have sustained contribution to control the terminal excitability.

4.3.2 KCNQ is important for constant AP waveform of calyx during high-frequency firing

The calyx of Held is capable of firing at very high frequency. Even in the early developmental stage (P2-3), *in vivo* recording detected a 150 Hz spontaneous firing rate of the calyx of Held in mice. With an increase in age, the spontaneous firing rate further

elevates and reaches above 300 Hz at P8 (Sierksma and Borst, 2017b). The high-frequency firing in calyx has remarkable physiological importance. It is critical for the auditory brainstem to encode timing with sub-millisecond accuracy for sound localization (Trussell, 1997). To test the contribution of KCNQ channels in high-frequency firing, we applied stimulation at different frequencies to generate AP trains in the calyx. In our experiments, the calyx could continuously fire at 333 Hz to generate 400 spikes without any failure. However, unlike MFBs, we observed a relatively constant AP waveform throughout the AP trains (Fig. 4.2). In the MFBs, the broadening of half-width for the 400th spike comparing to the 1st spike at 100 Hz stimulation was above 250% (Geiger and Jonas, 2000), whereas in the calyx the maximal broadening of AP at 100 Hz was $18.9\% \pm 7.5\%$. Even when the firing frequency was increased to 333 Hz, the maximal broadening was still below 100%. This suggests that the stable AP waveform for high-frequency firing is strongly related to the certain function of the calyx-MNTB synapse in auditory system.

The constant AP waveform associated with high-frequency activity is maintained by the hyperpolarization of ISP, which depends on the slow activation of KCNQ channels (Fig. 4.3). ISP is constituted by the afterpotential succeeding each spike during high-frequency firing. A typical afterpotential in calyx exhibits a depolarizing phase that raises the membrane potential from a fast afterhyperpolarization (fAHP) to near, but not over, -60 mV. (Kim, Kushmerick and von Gersdorff, 2010b). Interestingly, we showed that KCNQ channels play a significant role in regulating the ISP during high-frequency firing. Blocking KCNQ with XE991 led to the afterpotential following each spike becoming more positive as the time of high-frequency firing was prolonged, which overall impaired the hyperpolarization of the ISP. The impairment became more evident in the later phase of high-frequency firing, indicated by a

cumulative opening of KCNQ channels that was induced by the repetitive activation. Accompanying the depolarization of ISP, we observed a loss of constant AP waveform during high-frequency firing. The importance of ISP in regulating AP waveform during high-frequency firing was further demonstrated by injecting hyperpolarizing bias current. This type of current partially rescues the depolarization of ISP, at the same time partially rescuing the waveform change in the later phase of high-frequency firing. However, the hyperpolarized afterpotential itself could also inhibit the generation of the next spike by back-propagating to the axon (Paradiso and Wu, 2009). In our study, the hyperpolarizing current generated by KCNQ during high-frequency firing is not able to inhibit the generation of the next AP.

The hyperpolarized ISP has several important physiological consequences. Our data showed that the hyperpolarized ISP prevents the cumulative inactivation of NaV channels and Kv1 channels. We detected larger Na⁺ as well as Kv1 currents under the control template comparing with the XE991 command template, which suggests that more Na⁺ and Kv1 channels are available to open with the activation of KCNQ channels. Na⁺ channels are capable of shaping the AP in multiple ways, which is highly dependent on the timing of Na⁺ current generation. For example, the transient Na⁺ current shapes the depolarization phase of the AP, whereas the resurgent sodium current shapes the DAP (Brody and Yue, 2000; Kim et al., 2010a). Reduction in the number of Na⁺ channels could decrease the amplitude of AP and DAP. The Kv1 channel is crucial to shaping the half-width of APs during high-frequency firing (Geiger and Jonas, 2000). We took advantage of our naïve waveform, directly detecting the change of Na⁺ and Kv1 current which provided additional support for the previous conclusions. In the meanwhile, we demonstrated that not only fast-activating ion channels, but also slow-activating ion channels, such as KCNQ, are also important for regulating the shape of

APs during high-frequency firing. They are not directly regulating, but act by affecting other fast-activating ion channels.

4.3.3 Impact of AP waveforms on calcium influx during high-frequency firing

The shape of the AP is the most important determinant affecting the calcium charge transfer. Using the naïve 333 Hz AP trains, we were able to detect the calcium current change during high-frequency firing, and the important role that KCNQ channels play in regulating calcium current change. We found that in the control condition, the slight change of AP shape (a minor decrease in amplitude and increase in half-width) during high-frequency firing induced a subtle reduction of the calcium amplitude, yet a subtle elevation of total calcium charge as the number of spike increases (Fig. 4.7 B). This result is consistent with the previous observation in MFB (Geiger and Jonas, 2000). Change of AP waveform can affect the calcium current in multiple ways. The depolarization phase of AP selectively determines the total number of recruited VGCCs, while the repolarization phase controls both the number and kinetics of activated VGCCs (Yang, 2006b). It was also reported that the change in driving force for calcium entry could be canceled out by the change in calcium channels gating during afterpotential in the calyx of Held (Clarke et al., 2016). In general, we observed a relative constant calcium charge transfer evoked by the control command template regarding the amplitude and area integral.

The function of KCNQ channels in stabilizing calcium current becomes obviously crucial as the time of high-frequency firing is prolonged. When the magnitude of AP waveform change increased to the later phase of XE991 command template, it no longer induced a rise but instead led to a significant decrease of total

calcium charge transfer as shown in Fig. 4.7B. One possible explanation for the decline in overall calcium current is due to the APs not being able to evoke all subtypes of VGCCs in the calyx of Held, which has multiple subtypes of VGCCs including P/Q-type, N-type and R-type (Borst and Soria van Hoeve, 2012; Wu et al., 1998, 1999). Some subtypes, such as N-type VGCC, have relative a positive activation threshold that required the membrane potential to be depolarized to at least -30 mV to evoke the current (Wu et al., 1999). However, the peak of APs in the later phase of the XE991 command template decreased to ~ -40 mV, which is insufficient to activate N-type VGCCs (Fig. 4.7A). In the calyx of Held, the P/Q-type VGCC is responsible for inducing the majority calcium inflow and effectively triggering glutamate release (Wu et al., 1999). Interestingly, depolarizing pulses below the apparent activation range of P/Q-type VGCCs, which is around -45 to -50 mV, are still capable of causing an elevation of intracellular calcium level in the calyx of Held (Awatramani et al., 2005). Although N-type VGCCs and R-type VGCCs are also expressed in the calyx, they are less efficient to trigger glutamate release due to their relatively greater distance from the glutamate release sites (Inchauspe et al., 2007). Whether low-voltage-activated Ca^{2+} channels, T-type Ca^{2+} channels, are expressed in the calyx of Held still needs to be determined (Iwasaki and Takahashi, 1998b; Wu et al., 1998).

The total amount of calcium is more important than the peak of calcium current to govern the neurotransmitter release (Clarke et al., 2016). A decrease in the total amount of calcium can induce a decrease of EPSC, suggesting a decreasing of glutamate released from the presynaptic terminal (Hori and Takahashi, 2009b). In consequence, constant calcium current during high-frequency firing can induce constant glutamate release and further ensure the reliability of high-frequency signal transmission. Given the key role of KCNQ channels in stabilizing the calcium current by affecting the AP

waveform during high-frequency firing, we conclude that KCNQ channels contribute to reliable high-frequency signal transmission. However, KCNQ channels are one of the ion channels responsible for hyperpolarizing the RMP of the calyx of Held. It is known that a small depolarization of RMP can increase the background level of calcium and further enhances the glutamate release at the calyceal terminal (Awatramani et al., 2005). Increases in EPSCs was indeed observed after blocking KCNQ channels as we reported previously, suggesting an increase of overall glutamate release from the presynaptic terminal. It is possible that KCNQ channels play comprehensive and distinct roles in controlling the Ca^{2+} current for resting and firing conditions, respectively, that would have an overall complex effect on the glutamate releases. Comparing the EPSCs before and after blocking KCNQ channels during prolonged high-frequency stimulation would be beneficial to allow interpretation of the comprehensive functions of KCNQ on glutamate release.

CHAPTER 5. CONCLUSION AND PERSPECTIVES

5.1 Conclusion

Sound localization is the ability to recognize direction and estimate the distance of a sound source. Neurons of the auditory system are able to distinguish binaural signals with sub-millisecond accuracy; this characteristic enables them to identify the source of a sound precisely. As a result, they are specialized to fire with high frequency (up to hundreds of hertz), as well as transmit the signals with high fidelity. The MNTB is a key inverting relay in the auditory brainstem and takes part in sound localization by providing the downstream nucleus inhibitory signals to calculate IDT and IIT, which are two important cues for sound localization. Each principal neuron in MNTB receives a single input from the contralateral global bushy cell via a giant axosomatic terminal, the calyx of Held. Varieties of presynaptic and postsynaptic mechanisms have been found for regulating the reliable high-frequency signal transmission, including the expression of different types of K^+ channels. Several K^+ channels that have been well-characterized in the calyx-MNTB synapse. Each specific type of K^+ channel contributes toward preserving the temporal pattern of firing at high frequency with their unique properties. Given the significant roles that K^+ channels have in the calyx-MNTB synapse, I focused on identifying and investigating the important physiological functions of two different types of K^+ channels, postsynaptic SK channels and

presynaptic KCNQ channels in the calyx-MNTB synapse. Using whole-cell patch-clamp recording, I investigated the properties of SK channels and KCNQ channels and illustrated how they participated in reliably transmitting the high-frequency signals in the calyx-MNTB synapse with their different subcellular localization.

Although both SK channels and KCNQ channels selectively mediate K^+ charger transfer and the openings lead to hyperpolarization of membrane potential in the calyx-MNTB synapse, they have different activation mechanisms and properties. SK channels mediated both a transient spontaneous current and a tonic current in MNTB neurons. The activation of SK channels required cytosolic Ca^{2+} sources. Several types of Ca^{2+} sources in the MNTB neurons are involved in activating the SK channels. Ca^{2+} released from internal Ca^2 stores form Ca^{2+} sparks that transiently activate the SK channels to generate the STOCs, while the Ca^{2+} influx from the VGCCs and NMDARs are capable of evoking the tonic SK current. SK channels have high sensitivity to the changes in intracellular Ca^{2+} concentrations. They can be activated by sub-micromolar concentrations of cytosolic Ca^{2+} and open with a time constant of 5-15 ms. In contrast, KCNQ channels are voltage-gated K^+ channels and present in the calyx of Held. The activation of KCNQ channels solely depends on the change of membrane potential. KCNQ channels mediate a tonic current in the calyx of Held with a slow-activating (time constant for the fast component is 35 ms and the slow component is 308 ms) and non-inactivating kinetics.

Understanding the activation mechanism and kinetics of ion channels assists us to better investigate their potential function in this synapse. Both SK channels and KCNQ channels have relative hyperpolarizing activation thresholds, which are below the RMP of their subcellular localization. As a result, SK channels and KCNQ channels participate in affecting the resting membrane potential and conductance of the MNTB

neuron and the calyx of Held, respectively. Additionally, both SK channels and KCNQ channels can be activated during action potentials which in turn regulate the firing activities of the calyx-MNTB synapse, though with differential physiological consequences. SK channels control the afterpotential and limit MNTB neuronal excitability by preventing the generation of aberrant APs during high-frequency firing. The effect of SK channels to the one-to-one signal transmission from the presynaptic calyces to the postsynaptic MNTB neurons is postsynaptic independent. The relatively slow kinetics allow SK current summation during high-frequency firing, thus counteracting the afterdepolarization and stabilizing the overall excitability. Nevertheless, the high-frequency firing in the calyx of Held induced a cumulative activation of KCNQ channels. As a consequence, it produced a sustained and gradually increase hyperpolarizing current during high-frequency firing that is critical for the calyx to reduce membrane excitability and maintain the AP waveform, especially in the later phase of high-frequency firing. The uniform waveform of AP ensures that the calyceal terminals repetitively trigger constant calcium current, which guarantees the reliable presynaptic mechanism for glutamate transmission.

Overall, with the existence of SK channels in the postsynaptic component and KCNQ channels in the presynaptic component, this calyx-MNTB synapse transmits the high-frequency signal with increasing reliability.

5.2 Future perspectives

5.2.1 The physiological function of STOCs

STOCs, also called small miniature outward currents (SMOCs) in some previous studies, are widely expressed in various types of cells including smooth muscle cells, cardiac myocytes, and neurons (Cui, 2004; Driessen et al., 2010; Klement et al., 2010; Saito and Yanagawa, 2013; Satin and Adams, 1987). Over years of studies, the generation and regulation mechanisms of STOCs have become increasingly clear. The generation of STOCs is highly dependent on Ca^{2+} -induced Ca^{2+} release (CICR), by which calcium is released from the ryanodine receptors on the ER. Basically, Ca^{2+} entering through VGCCs induces the Ca^{2+} release from the internal store via ryanodine receptors, further triggering the Ca^{2+} -activated K^+ channel to initiate STOC. However, in addition to the pathway I identified in MNTB neurons, other specialized mechanisms are also adopted for the activation of STOCs. For example, it has been shown that big conductance Ca^{2+} -activated K^+ (BK) channels are also involved in the generation of STOCs (Irie and Trussell, 2017; Mitra and Slaughter, 2002). Furthermore, in addition to R-type VGCC, diverse types of VGCCs such as P/Q-type, L-type, and T-type VGCCs, have been reported to supply the Ca^{2+} for the opening of ryanodine receptors and to further activate STOCs (Cui, 2004; Irie and Trussell, 2017; Mitra and Slaughter, 2002).

The functional significance of STOCs in MNTB neurons requires additional investigation. Some previous studies reported that the STOCs are important in regulating the firing pattern. For example, in midbrain dopamine neuron, inhibiting the generation of SMOCs by depleting internal Ca^{2+} sources with amphetamine changes the irregular firing pattern to a regular firing pattern and increases the firing rate; recordings from the cartwheel cell have shown that blocking CICR with ryanodine switches the firing pattern from simple-firing to burst firing (Cui, 2004; Irie and Trussell, 2017). It is the important to identify the physiological function of STOCs in

MNTB neurons. Two independent lines of evidence suggest that STOCs have functional significance in MNTB neurons. First, *in vivo* recordings show that MNTB neurons also displays robust spontaneous firing activity and generate bursts of action potentials before hearing onset, although MNTB neurons in the brain slice rarely have spontaneously firing (Tritsch et al., 2010). Spontaneous activities are important for MNTB neurons to establish the precise topographic organization (Leao et al., 2006). Second, STOCs appear in early postnatal days, are sustained during the critical developmental period, and gradually decline after hearing onset. It is plausible that STOCs are specifically generated before hearing onset to regulate the firing pattern of MNTB neurons, which further ensures the precise topographic organization of the MNTB neurons. This hypothesis will be tested in future *in vivo* studies.

5.2.2 Role of presynaptic KCNQ channels in the conventional synapse

The calyx of Held is the largest synapse in vertebrates. Its substantial size allows for direct patch-clamp recording, which solved the technical difficulty limiting research on the presynaptic terminal. Over decades, the calyx of Held has been well studied as a model system for investigating the ion channels of presynaptic terminals and fast glutamatergic transmission, and provides critical information regarding the conventional synapse. However, the calyx of Held is specialized for fulfilling the task of sound localization with characteristics such as phase locking, firing APs at extremely high frequency, and high-fidelity of signal transmission. In the calyx of Held, I found that KCNQ channels are required to maintain the constant AP waveform during the high-frequency firing, which ensures the reliable high-frequency signal transmission in a presynaptic mechanism. KCNQ channels are also highly expressed in conventional

synapses such as those in the hippocampus (Chung et al., 2006; Cooper et al., 2000b). Therefore, I would assume that KCNQ channels play an important role in shaping the AP waveform in the conventional synapses as well. It is important to notice that presynaptic terminal and signal transmission in conventional synapses such as in the hippocampus have some different properties compared with the calyceal terminal. For example, one type of presynaptic terminal, the mossy fiber bouton, which connects with the hippocampal CA3 pyramidal neurons, has activity-dependent AP broadening and fires at low frequency (gamma oscillations : 30–90 Hz; theta oscillations: 3–8 Hz), which differs from the calyx of Held (Delvendahl et al., 2013; Geiger and Jonas, 2000). Accordingly, blocking KCNQ channels might lead to different physiological consequences. Understanding the function of KCNQ channels in conventional synapses will not only complete our knowledge about their function at the level of the neuronal network, but will also provide a new insight into the structure-function relationship of KCNQ channels.

5.2.3 Diseases related to SK channels and KCNQ channels

Given that the available results from my studies on SK channels and KCNQ channels suggest that both channel types indeed play important functions in the reliable high-frequency signal transmission in this calyx-MNTB synapse, it is plausible that they directly affect the function of the MNTB in sound localization. The significant roles of the MNTB in sound localization have been demonstrated in clinical studies that have found that patients with a lesion in the trapezoid body have an impaired ability to detect the sound movement (Furst et al., 2000; Geiger and Jonas, 2000).

Furthermore, both the SK channels and KCNQ channels are widely distributed in the central nervous system. Malfunctions of these channels have been reported to be involved in multiple brain diseases. For example, alteration of SK activity in prefrontal neurons is related to cognitive deficits in Alzheimer's disease (Proulx et al., 2015), and the activity of KCNQ channels contributes to hippocampus-dependent spatial memory (Peters et al., 2004). Fundamentally mechanistic study of SK channels and KCNQ channels might shed light on the development of new therapeutic treatments to cure these diseases. Additionally, mutations in KCNQ channels are implicated in human diseases, including deafness, epilepsy, and autism spectrum disorders (ASDs) (Biervert et al., 1998; Charlier et al., 1998; Gilling et al., 2013; Jentsch, 2000). It is important to note that deficits in sound localization have been found in a group of autistic patients (Teder-Sälejärvi et al., 2005; Visser et al., 2013). However, the internal relationship between the KCNQ mutation and its effect on sound localization in ASDs is not clear. Further investigation of KCNQ channels with mouse models might provide the explanation for this symptom in ASDs.

REFERENCES

- Adams, P.R., and Brown, D.A. (1980). Bullfrog Sympathetic Neurones. 353–355.
- Adelman, J.P., Maylie, J., and Sah, P. (2012a). Small-Conductance Ca²⁺-Activated K⁺ Channels: Form and Function. *Annu. Rev. Physiol.* 74, 245–269.
- Adelman, J.P., Maylie, J., and Sah, P. (2012b). Small-Conductance Ca²⁺-Activated K⁺ Channels: Form and Function. *Annu. Rev. Physiol.* 74, 245–269.
- Awatramani, G.B., Price, G.D., and Trussell, L.O. (2005). Modulation of Transmitter Release by Presynaptic Resting Potential and Background Calcium Levels. 48, 109–121.
- Azevedo, F.A.C., Carvalho, L.R.B., Grinberg, L.T., Farfel, J.M., Ferretti, R.E.L., Leite, R.E.P., Filho, W.J., Lent, R., and Herculano-Houzel, S. (2009). Equal numbers of neuronal and nonneuronal cells make the human brain an isometrically scaled-up primate brain. *J. Comp. Neurol.* 513, 532–541.
- Barnes-Davies, M., Owens, S., and Forsythe, I.D. (2001). Calcium channels triggering transmitter release in the rat medial superior olive. *Hear. Res.* 162, 134–145.
- Bean, B.P. (2007). The action potential in mammalian central neurons. 8, 18–20.
- Berntson, A.K., and Walmsley, B. (2008). Characterization of a potassium-based leak conductance in the medial nucleus of the trapezoid body. *Hear. Res.* 244, 98–106.
- Bevan, M.D., and Wilson, C.J. (1999). Mechanisms underlying spontaneous oscillation and rhythmic firing in rat subthalamic neurons. *J. Neurosci.* 19, 7617–7628.
- Biervert, C., Schroeder, B.C., Kubisch, C., Berkovic, S.F., Propping, P., Jentsch, T.J.,

- and Steinlein, O.K. (1998). A potassium channel mutation in neonatal human epilepsy. *Science* (80-.). 279, 403–406.
- Borst, J.G., and Sakmann, B. (1999). Effect of changes in action potential shape on calcium currents and transmitter release in a calyx-type synapse of the rat auditory brainstem. *Philos. Trans. R. Soc. Lond. B. Biol. Sci.* 354, 347–355.
- Borst, J.G.G., and Sakmann, B. (1996). Calcium influx and transmitter release in a fast CNS synapse. *Nature* 383, 431–434.
- Borst, J.G.G., and Sakmann, B. (1998). Calcium current during a single action potential in a large presynaptic terminal of the rat brainstem. *J. Physiol.* 506, 143–157.
- Borst, J.G.G., and Soria van Hoeve, J. (2012). The Calyx of Held Synapse: From Model Synapse to Auditory Relay. *Annu. Rev. Physiol.* 74, 199–224.
- Borst, J.G., Helmchen, F., and Sakmann, B. (1995). Pre- and postsynaptic whole-cell recordings in the medial nucleus of the trapezoid body of the rat. *J. Physiol.* 489 (Pt 3, 825–840.
- Boudreau, J.C., and Tsuchitani, C. (1968). Binaural interaction in the cat superior olive S segment. *J. Neurophysiol.* 31, 442–454.
- Brew, H.M., and Forsythe, I.D. (1995). Two voltage-dependent K⁺ conductances with complementary functions in postsynaptic integration at a central auditory synapse. *J. Neurosci.* 15, 8011–8022.
- Brody, D.L., and Yue, D.T. (2000). Release-independent short-term synaptic depression in cultured hippocampal neurons. *J. Neurosci.* 20, 2480–2494.
- Brown, D.A., and Passmore, G.M. (2009). Neural KCNQ (Kv7) channels. *Br. J. Pharmacol.* 156, 1185–1195.
- Brown, D.A., Marrion, N. V, and Smart, T.G. (1989). On the transduction mechanism for muscarine-induced inhibition of M-current in cultured rat sympathetic neurones. *J.*

Physiol. 413, 469–488.

Bucher, D., and Goaillard, J.M. (2011). Beyond faithful conduction: Short-term dynamics, neuromodulation, and long-term regulation of spike propagation in the axon. *Prog. Neurobiol.* 94, 307–346.

Burger, R.M., Forsythe, I.D., and Kopp-Scheinflug, C. (2015). Editorial: Inhibitory function in auditory processing. *Front. Neural Circuits* 9, 45.

Caminos, E., Garcia-Pino, E., Martinez-Galan, J.R., and Juiz, J.M. (2007). The potassium channel KCNQ5/Kv7.5 is localized in synaptic endings of auditory brainstem nuclei of the rat. *J. Comp. Neurol.* 505, 363–378.

Chandy, K.G., Fantino, E., Wittekindt, O., Kalman, K., Tong, L.L., Ho, T.H., Gutman, G.A., Crocq, M.A., Ganguli, R., Nimgaonkar, V., et al. (1998). Isolation of a novel potassium channel gene hSKCa3 containing a polymorphic CAG repeat: a candidate for schizophrenia and bipolar disorder? *Mol. Psychiatry* 3, 32–37.

Charlier, C., Singh, N. a, Ryan, S.G., Lewis, T.B., Reus, B.E., Leach, R.J., and Leppert, M. (1998). A pore mutation in a novel KQT-like potassium channel gene in an idiopathic epilepsy family. *Nat. Genet.* 18, 53–55.

Chen, X., Xue, B., Wang, J., Liu, H., Shi, L., and Xie, J. (2017). Potassium Channels: A Potential Therapeutic Target for Parkinson's Disease. *Neurosci. Bull.*

Chung, H.J., Jan, Y.N., and Jan, L.Y. (2006). Polarized axonal surface expression of neuronal KCNQ channels is mediated by multiple signals in the KCNQ2 and KCNQ3 C-terminal domains. *Proc. Natl. Acad. Sci.* 103, 8870–8875.

Clarke, S.G., Scarnati, X.M.S., and Paradiso, X.K.G. (2016). Neurotransmitter Release Can Be Stabilized by a Mechanism That Prevents Voltage Changes Near the End of Action Potentials from Affecting Calcium Currents. 36, 11559–11572.

Clause, A., Kim, G., Sonntag, M., Weisz, C.J.C., Vetter, D.E., Rubsamen, R., and

- Kandler, K. (2014). The Precise Temporal Pattern of Prehearing Spontaneous Activity Is Necessary for Tonotopic Map Refinement. *Neuron* 82, 822–835.
- Cooper, E.C., Aldape, K.D., Abosch, A., Barbaro, N.M., Berger, M.S., Peacock, W.S., Jan, Y.N., and Jan, L.Y. (2000a). Colocalization and coassembly of two human brain M-type potassium channel subunits that are mutated in epilepsy. *Proc. Natl. Acad. Sci. U. S. A.* 97, 4914–4919.
- Cooper, E.C., Aldape, K.D., Abosch, A., Barbaro, N.M., Berger, M.S., Peacock, W.S., Jan, Y.N., and Jan, L.Y. (2000b). Colocalization and coassembly of two human brain M-type potassium channel subunits that are mutated in epilepsy. *Proc. Natl. Acad. Sci. U. S. A.* 97, 4914–4919.
- Cooper, E.C., Harrington, E., Jan, Y.N., and Jan, L.Y. (2001). M channel KCNQ2 subunits are localized to key sites for control of neuronal network oscillations and synchronization in mouse brain. *J Neurosci* 21, 9529–9540.
- Cui, G. (2004). Spontaneous Opening of T-Type Ca²⁺ Channels Contributes to the Irregular Firing of Dopamine Neurons in Neonatal Rats. *J. Neurosci.* 24, 11079–11087.
- Cuttle, M.F., Rusznák, Z., Wong, A.Y.C., Owens, S., and Forsythe, I.D. (2001). Modulation of a presynaptic hyperpolarization-activated cationic current (I_h) at an excitatory synaptic terminal in the rat auditory brainstem. *J. Physiol.* 534, 733–744.
- Davoren, J.E., Claffey, M.M., Snow, S.L., Reese, M.R., Arora, G., Butler, C.R., Boscoe, B.P., Chenard, L., Deninno, S.L., Drozda, S.E., et al. (2015). Discovery of a novel Kv7 channel opener as a treatment for epilepsy. *Bioorganic Med. Chem. Lett.* 25, 4941–4944.
- Delmas, P., and Brown, D.A. (2005). Pathways modulating neural KCNQ/M (Kv7) potassium channels. *Nat. Rev. Neurosci.* 6, 850–862.
- Delvendahl, I., Weyhersmüller, A., Ritzau-Jost, A., and Hallermann, S. (2013).

- Hippocampal and cerebellar mossy fibre boutons – same name, different function. *J. Physiol.* *591*, 3179–3188.
- Deutch, A.Y. (2013). Chapter 6 - Neurotransmitters A2 - Squire, Larry R. D. Berg, F.E. Bloom, S. du Lac, A. Ghosh, and N.C.B.T.-F.N. (Fourth E. Spitzer, eds. (San Diego: Academic Press), pp. 117–138.
- Dodson, P.D., and Forsythe, I.D. (2004). Presynaptic K⁺ channels: electrifying regulators of synaptic terminal excitability. *27*.
- Dodson, P.D., Barker, M.C., and Forsythe, I.D. (2002). Two heteromeric Kv1 potassium channels differentially regulate action potential firing. *J. Neurosci.* *22*, 6953–6961.
- Dodson, P.D., Billups, B., Rusznák, Z., Szucs, G., Barker, M.C., and Forsythe, I.D. (2003). Presynaptic Rat Kv1.2 Channels Suppress Synaptic Terminal Hyperexcitability Following Action Potential Invasion. *J. Physiol.* *550*, 27–33.
- Driessen, R., Galajda, P., Keymer, J.E., Dekker, C., Jiang, H., Xia, D., Savarino, S.J., Bullitt, E., Spring, S., Opitz, D., et al. (2010). Monday, February 22, 2010. 2010.
- Edgerton, J.R., and Reinhart, P.H. (2003). Distinct contributions of small and large conductance Ca²⁺-activated K⁺ channels to rat Purkinje neuron function. *J. Physiol.* *548*, 53–69.
- Engel, D., Jonas, P., Institut, P., and Freiburg, D.U. (2005). Presynaptic Action Potential Amplification by Voltage-Gated Na⁺ Channels in Hippocampal Mossy Fiber Boutons. *45*, 405–417.
- Ford, M.C., Grothe, B., and Klug, A. (2009). Fenestration of the calyx of held occurs sequentially along the tonotopic axis, is influenced by afferent activity, and facilitates glutamate clearance. *J. Comp. Neurol.* *514*, 92–106.
- Forsythe, I.D. (1994). Direct patch recording from identified presynaptic terminals

mediating glutamatergic EPSCs in the rat CNS, in vitro. *J. Physiol.* 479 (Pt 3, 381–387.

Forsythe, I.D., and Barnes-Davies, M. (1993). The Binaural Auditory Pathway: Excitatory Amino Acid Receptors Mediate Dual Timecourse Excitatory Postsynaptic Currents in the Rat Medial Nucleus of the Trapezoid Body. *Proc. R. Soc. B Biol. Sci.* 251, 151–157.

Friauf, E. (1992). Tonotopic Order in the Adult and Developing Auditory System of the Rat as Shown by c-fos Immunocytochemistry. *Eur. J. Neurosci.* 4, 798–812.

Furst, M., Aharonson, V., Levine, R.A., Fullerton, B.C., Tadmor, R., Pratt, H., Polyakov, A., and Korczyn, A.D. (2000). Sound lateralization and interaural discrimination. Effects of brainstem infarcts and multiple sclerosis lesions. *Hear. Res.* 143, 29–42.

GARDOS, G. (1958). The function of calcium in the potassium permeability of human erythrocytes. *Biochim. Biophys. Acta* 30, 653–654.

Gazula, V., Strumbos, J., and Mei, X. (2010). Localization of Kv1. 3 channels in presynaptic terminals of brainstem auditory neurons. *J. ...* 518, 3205–3220.

Geiger, J.R.P., and Jonas, P. (2000). Dynamic control of presynaptic Ca²⁺ inflow by fast-inactivating K⁺ channels in hippocampal mossy fiber boutons. *Neuron* 28, 927–939.

Gilling, M., Rasmussen, H.B., Calloe, K., Sequeira, A.F., Baretto, M., Oliveira, G., Almeida, J., Lauritsen, M.B., Ullmann, R., Boonen, S.E., et al. (2013). Dysfunction of the Heteromeric K(V)7.3/K(V)7.5 Potassium Channel is Associated with Autism Spectrum Disorders. *Front. Genet.* 4, 54.

Greene, D.L., and Hoshi, N. (2016). Modulation of Kv7 channels and excitability in the brain. *Cell. Mol. Life Sci.*

- Greene, D.L., and Hoshi, N. (2017). Modulation of Kv7 channels and excitability in the brain. *Cell. Mol. Life Sci.* 74, 495–508.
- Gribkoff, V.K. (2003). The therapeutic potential of neuronal KCNQ channel modulators. *Expert Opin. Ther. Targets* 7, 737–748.
- Grothe, B. (2003). New roles for synaptic inhibition in sound localization. *Nat. Rev. Neurosci.* 4, 540–550.
- Haley, J.E., Abogadie, F.C., Delmas, P., Dayrell, M., Vallis, Y., Milligan, G., Caulfield, M.P., Brown, D. a, and Buckley, N.J. (1998). The alpha subunit of Gq contributes to muscarinic inhibition of the M-type potassium current in sympathetic neurons. *J. Neurosci.* 18, 4521–4531.
- Hallworth, N.E., Wilson, C.J., and Bevan, M.D. (2003). Apamin-Sensitive Small Conductance Calcium-Activated Potassium Channels, through their Selective Coupling to Voltage-Gated Calcium Channels, Are Critical Determinants of the Precision, Pace, and Pattern of Action Potential Generation in Rat Subthalamic Nu. *J. Neurosci.* 23, 7525–7542.
- Hamann, M., Billups, B., and Forsythe, I.D. (2003). Non-calyceal excitatory inputs mediate low ® delity synaptic transmission in rat auditory brainstem slices. *Eur. J. Neurosci.* 18, 2899–2903.
- Hammond, R.S. (2006). Small-Conductance Ca²⁺-Activated K⁺ Channel Type 2 (SK2) Modulates Hippocampal Learning, Memory, and Synaptic Plasticity. *J. Neurosci.* 26, 1844–1853.
- Hee Kim, J., Kushmerick, C., and von Gersdorff, H. (2010a). Presynaptic Resurgent Na⁺ Currents Sculpt the Action Potential Waveform and Increase Firing Reliability at a CNS Nerve Terminal. *J. Neurosci.* 30, 15479–15490.
- Hee Kim, J., Kushmerick, C., and von Gersdorff, H. (2010b). Presynaptic Resurgent

- Na⁺ Currents Sculpt the Action Potential Waveform and Increase Firing Reliability at a CNS Nerve Terminal. *J. Neurosci.* *30*, 15479–15490.
- Hoffpauir, B.K. (2006). Synaptogenesis of the Calyx of Held: Rapid Onset of Function and One-to-One Morphological Innervation. *J. Neurosci.* *26*, 5511–5523.
- Hoffpauir, B.K., Kolson, D.R., Mathers, P.H., and Spirou, G.A. (2010). Maturation of synaptic partners: functional phenotype and synaptic organization tuned in synchrony. *J. Physiol.* *588*, 4365–4385.
- Hori, T., and Takahashi, T. (2009a). Mechanisms underlying short-term modulation of transmitter release by presynaptic depolarization. *J. Physiol.* *587*, 2987–3000.
- Hori, T., and Takahashi, T. (2009b). Mechanisms underlying short-term modulation of transmitter release by presynaptic depolarization. *J. Physiol.* *587*, 2987–3000.
- Howard, R.J., Clark, K.A., Holton, J.M., and Minor, D.L. (2007). Structural Insight into KCNQ (Kv7) Channel Assembly and Channelopathy. *Neuron* *53*, 663–675.
- Hu, H., Vervaeke, K., and Storm, J.F. (2007). M-Channels (Kv7/KCNQ Channels) That Regulate Synaptic Integration, Excitability, and Spike Pattern of CA1 Pyramidal Cells Are Located in the Perisomatic Region. *J. Neurosci.* *27*, 1853–1867.
- Huang, H., and Trussell, L.O. (2008). Control of Presynaptic Function by a Persistent Na⁺ Current. *Neuron* *60*, 975–979.
- Huang, H., and Trussell, L.O. (2011). KCNQ5 channels control resting properties and release probability of a synapse. *Nat. Neurosci.* *14*, 840–847.
- Ikonen, S., and Riekkinen, P. (1999). Effects of apamin on memory processing of hippocampal-lesioned mice. *Eur. J. Pharmacol.* *382*, 151–156.
- Imbrici, P., Camerino, D.C., and Tricarico, D. (2013). Major channels involved in neuropsychiatric disorders and therapeutic perspectives. *Front. Genet.* *4*, 1–19.
- Inchauspe, C.G., Forsythe, I.D., and Uchitel, O.D. (2007). Changes in synaptic

- transmission properties due to the expression of N-type calcium channels at the calyx of Held synapse of mice lacking P/Q-type calcium channels. *J. Physiol.* 584, 835–851.
- Irie, T., and Trussell, L.O. (2017). Double-Nanodomain Coupling of Calcium Channels, Ryanodine Receptors, and BK Channels Controls the Generation of Burst Firing. *Neuron* 96, 856–870.e4.
- Ishikawa, T., Nakamura, Y., Saitoh, N., Li, W.-B., Iwasaki, S., and Takahashi, T. (2003). Distinct roles of Kv1 and Kv3 potassium channels at the calyx of Held presynaptic terminal. *J. Neurosci.* 23, 10445–10453.
- Iwasaki, S., and Takahashi, T. (1998a). Developmental changes in calcium channel types mediating synaptic transmission in rat auditory brainstem. *J. Physiol.* 509, 419–423.
- Iwasaki, S., and Takahashi, T. (1998b). Developmental changes in calcium channel types mediating synaptic transmission in rat auditory brainstem. *J. Physiol.* 509 (Pt 2, 419–423.
- Jackson, M.B., Konnerth, a, and Augustine, G.J. (1991). Action potential broadening and frequency-dependent facilitation of calcium signals in pituitary nerve terminals. *Proc. Natl. Acad. Sci. U. S. A.* 88, 380–384.
- Jentsch, T.J. (2000). Neuronal KCNQ potassium channels: physiology and role in disease. *Nat. Rev. Neurosci.* 1, 21–30.
- Johnston, J., Griffin, S.J., Baker, C., Skrzypiec, A., Chernova, T., and Forsythe, I.D. (2008). Initial segment Kv2.2 channels mediate a slow delayed rectifier and maintain high frequency action potential firing in medial nucleus of the trapezoid body neurons. *J. Physiol.* 586, 3493–3509.
- Johnston, J., Forsythe, I.D., and Kopp-Scheinflug, C. (2010). Going native: voltage-gated potassium channels controlling neuronal excitability. *J. Physiol.* 588, 3187–3200.

- Joris, P.X., Carney, L.H., Smith, P.H., and Yin, T.C. (1994). Enhancement of neural synchronization in the anteroventral cochlear nucleus. I. Responses to tones at the characteristic frequency. *J. Neurophysiol.* *71*, 1022 LP-1036.
- Joshi, I. (2004). The Role of AMPA Receptor Gating in the Development of High-Fidelity Neurotransmission at the Calyx of Held Synapse. *J. Neurosci.* *24*, 183–196.
- Joshi, I., and Wang, L.-Y. (2002). Developmental profiles of glutamate receptors and synaptic transmission at a single synapse in the mouse auditory brainstem. *J. Physiol.* *540*, 861–873.
- Kandler, K., and Friauf, E. (1993). Pre- and postnatal development of efferent connections of the cochlear nucleus in the rat. *J. Comp. Neurol.* *328*, 161–184.
- Kandler, K., Clause, A., and Noh, J. (2009). Tonotopic reorganization of developing auditory brainstem circuits. *Nat. Neurosci.* *12*, 711–717.
- Kim, J.H., Sizov, I., Dobretsov, M., and von Gersdorff, H. (2007a). Presynaptic Ca²⁺ buffers control the strength of a fast post-tetanic hyperpolarization mediated by the $\alpha 3$ Na⁺/K⁺-ATPase. *Nat. Neurosci.* *10*, 196–205.
- Kim, J.H., Sizov, I., Dobretsov, M., and von Gersdorff, H. (2007b). Presynaptic Ca²⁺ buffers control the strength of a fast post-tetanic hyperpolarization mediated by the $\alpha 3$ Na⁺/K⁺-ATPase. *Nat. Neurosci.* *10*, 196–205.
- Klement, G., Druzin, M., Haage, D., Malinina, E., Århem, P., and Johansson, S. (2010). Spontaneous Ryanodine-Receptor-Dependent Ca²⁺ Activated K⁺ Currents and Hyperpolarizations in Rat Medial Preoptic Neurons. *J. Neurophysiol.* *103*, 2900–2911.
- Kramar, E.A. (2004). A Novel Mechanism for the Facilitation of Theta-Induced Long-Term Potentiation by Brain-Derived Neurotrophic Factor. *J. Neurosci.* *24*, 5151–5161.
- Kubisch, C., Schroeder, B.C., Friedrich, T., Lütjohann, B., El-Amraoui, A., Marlin, S., Petit, C., and Jentsch, T.J. (1999). KCNQ4, a novel potassium channel expressed in

sensory outer hair cells, is mutated in dominant deafness. *Cell* 96, 437–446.

Kuwabara, N., DiCaprio, R.A., and Zook, J.M. (1991). Afferents to the medial nucleus of the trapezoid body and their collateral projections. *J. Comp. Neurol.* 314, 684–706.

Laughlin, M.M., Heijden, M. Van Der, and Joris, P.X. (2008). How Secure Is In Vivo Synaptic Transmission at the Calyx of Held ? *J. Neurosci.* 28, 10206–10219.

Leao, R.N., Sun, H., Svahn, K., Berntson, A., Youssoufian, M., Paolini, A.G., Fyffe, R.E.W., and Walmsley, B. (2006). Topographic organization in the auditory brainstem of juvenile mice is disrupted in congenital deafness. *J. Physiol.* 571, 563–578.

Leao, R.N., Tan, H.M., and Fisahn, A. (2009). Kv7/KCNQ Channels Control Action Potential Phasing of Pyramidal Neurons during Hippocampal Gamma Oscillations In Vitro. *J. Neurosci.* 29, 13353–13364.

Leão, R.M., Kushmerick, C., Pinaud, R., Renden, R., Li, G.-L., Taschenberger, H., Spirou, G., Levinson, S.R., and Von Gersdorff, H. (2005). Cellular/Molecular Presynaptic Na Channels: Locus, Development, and Recovery from Inactivation at a High-Fidelity Synapse. *J. Neurosci.* 25, 3724–3738.

Leão, R.N., Leão, R.M., Da Costa, L.F., Rock Levinson, S., and Walmsley, B. (2008). A novel role for MNTB neuron dendrites in regulating action potential amplitude and cell excitability during repetitive firing. *Eur. J. Neurosci.* 27, 3095–3108.

Lee, S.Y., Choi, H.K., Kim, S.T., Chung, S., Park, M.K., Cho, J.H., Ho, W.K., and Cho, H. (2010). Cholesterol inhibits M-type K⁺ channels via protein kinase C-dependent phosphorylation in sympathetic neurons. *J. Biol. Chem.* 285, 10939–10950.

Li, W., Kaczmarek, L.K., and Perney, T.M. (2001). Localization of two high-threshold potassium channel subunits in the rat central auditory system. *J Comp Neurol* 437, 196–218.

Lorteije, J.A.M., Rusu, S.I., Kushmerick, C., and Borst, J.G.G. (2009). Reliability and

- Precision of the Mouse Calyx of Held Synapse. *J. Neurosci.* 29, 13770–13784.
- Marrion, N. V (1997). CONTROL OF M-CURRENT. 483–504.
- Maylie, J., Bond, C.T., Herson, P.S., Lee, W.S., and Adelman, J.P. (2004). Small conductance Ca²⁺-activated K⁺ channels and calmodulin. *J Physiol* 554, 255–261.
- McCormick, D.A. (2013). Chapter 5 - Membrane Potential and Action Potential A2 - Squire, Larry R. D. Berg, F.E. Bloom, S. du Lac, A. Ghosh, and N.C.B.T.-F.N. (Fourth E. Spitzer, eds. (San Diego: Academic Press), pp. 93–116.
- Ming, G., and Wang, L.-Y. (2003). Properties of voltage-gated sodium channels in developing auditory neurons of the mouse in vitro. *Chinese Med. Sci. J. = Chung-Kuo I Hsueh K'o Hsueh Tsa Chih* 18, 67–74.
- Mitra, P., and Slaughter, M.M. (2002). Mechanism of generation of spontaneous miniature outward currents (SMOCs) in retinal amacrine cells. *J. Gen. Physiol.* 119, 355–372.
- Nakamura, P.A., and Cramer, K.S. (2011). Formation and Maturation of the Calyx of Held. *Hear. Res.* 276, 70–78.
- Nakamura, Y., and Takahashi, T. (2007). Developmental changes in potassium currents at the rat calyx of Held presynaptic terminal. 3, 1101–1112.
- Paradiso, K., and Wu, L.-G. (2009). Small voltage changes at nerve terminals travel up axons to affect action potential initiation. *Nat. Neurosci.* 12, 541–543.
- Passmore, G.M., Selyanko, A.A., Mistry, M., Al-Qatari, M., Marsh, S.J., Matthews, E.A., Dickenson, A.H., Brown, T.A., Burbidge, S.A., Main, M., et al. (2003). KCNQ/M currents in sensory neurons: significance for pain therapy. *J. Neurosci.* 23, 7227–7236.
- Peters, H.C., Hu, H., Pongs, O., Storm, J.F., and Isbrandt, D. (2004). Conditional transgenic suppression of M channels in mouse brain reveals functions in neuronal excitability, resonance and behavior. *Nat. Neurosci.* 8, 51.

- Pfaffinger, P. (1988). Muscarine and t-LHRH suppress M-current by activating an IAP-insensitive G-protein. *J. Neurosci.* 8, 3343–3353.
- Proulx, E., Fraser, P., McLaurin, J., and Lambe, E.K. (2015). Impaired Cholinergic Excitation of Prefrontal Attention Circuitry in the TgCRND8 Model of Alzheimer's Disease. *J. Neurosci.* 35, 12779–12791.
- Puente, N., Azkue, J.J., and Don, F. (2003). SUBCELLULAR LOCALIZATION OF THE VOLTAGE-DEPENDENT POTASSIUM CHANNEL Kv3 . 1b IN POSTNATAL AND ADULT RAT. *118*, 889–898.
- Rodríguez-Contreras, A., de Lange, R.P.J., Lucassen, P.J., and Borst, J.G.G. (2006). Branching of calyceal afferents during postnatal development in the rat auditory brainstem. *J. Comp. Neurol.* 496, 214–228.
- Ryugo, D.K., and Spirou, G.A. (2010). Auditory System: Giant Synaptic Terminals, Endbulbs, and Calyces. *Encycl. Neurosci.* 759–770.
- Sabatini, B.L., and Regehr, W.G. (1997). Control of Neurotransmitter Release by Presynaptic Waveform at the Granule Cell to Purkinje Cell Synapse. *17*, 3425–3435.
- Sailer, C.A., Kaufmann, W.A., Marksteiner, J., and Knaus, H.G. (2004). Comparative immunohistochemical distribution of three small-conductance Ca²⁺-activated potassium channel subunits, SK1, SK2, and SK3 in mouse brain. *Mol. Cell. Neurosci.* 26, 458–469.
- Saito, Y., and Yanagawa, Y. (2013). Ca²⁺-activated ion currents triggered by ryanodine receptor-mediated Ca²⁺ release control firing of inhibitory neurons in the prepositus hypoglossi nucleus. *J. Neurophysiol.* 109, 389–404.
- Sanguinetti, M.C., Curran, M.E., Zou, A., Shen, J., Specter, P.S., Atkinson, D.L., and Keating, M.T. (1996). Coassembly of KVLQT1 and minK (IsK) proteins to form cardiac IKS potassium channel. *Nature* 384, 80–83.

- Satin, L.S., and Adams, P.R. (1987). Spontaneous miniature outward currents in cultured bullfrog neurons. *Brain Res.* 401, 331–339.
- Sätzler, K., Söhl, L.F., Bollmann, J.H., Borst, J.G.G., Frotscher, M., Sakmann, B., Lübke, J.H.R., Satzler, K., Sohl, L.F., Bollmann, J.H., et al. (2002). Three-dimensional reconstruction of a calyx of Held and its postsynaptic principal neuron in the medial nucleus of the trapezoid body. *J. Neurosci.* 22, 10567–10579.
- Schneggenburger, R., and Forsythe, I.D. (2006). The calyx of Held. *Cell Tissue Res.* 326, 311–337.
- Schumacher, M.A., Rivard, A.F., Bächinger, H.P., and Adelman, J.P. (2001). Structure of the gating domain of a Ca²⁺-activated K⁺ channel complexed with Ca²⁺/calmodulin. *Nature* 410, 1120–1124.
- Sierksma, M.C., and Borst, J.G.G. (2017a). Resistance to action potential depression of a rat axon terminal in vivo. *Proc. Natl. Acad. Sci.* 114, 201619433.
- Sierksma, M.C., and Borst, J.G.G. (2017b). Resistance to action potential depression of a rat axon terminal in vivo. *Proc. Natl. Acad. Sci.* 114, 201619433.
- Sonntag, M., Englitz, B., Kopp-Scheinflug, C., and Rubsamen, R. (2009). Early Postnatal Development of Spontaneous and Acoustically Evoked Discharge Activity of Principal Cells of the Medial Nucleus of the Trapezoid Body: An In Vivo Study in Mice. *J. Neurosci.* 29, 9510–9520.
- Spiro, G. a, Brownell, W.E., and Zidanic, M. (1990). Recordings from cat trapezoid body and HRP labeling of globular bushy cell axons. *J. Neurophysiol.* 63, 1169–1190.
- Stackman, R.W., Hammond, R.S., Linardatos, E., Gerlach, A., Maylie, J., Adelman, J.P., and Tzounopoulos, T. (2002). Small conductance Ca²⁺-activated K⁺ channels modulate synaptic plasticity and memory encoding. *J. Neurosci.* 22, 10163–10171.
- Stocker, M., and Pedarzani, P. (2000). Differential Distribution of Three Ca²⁺-

Activated K⁺ Channel Subunits, SK1, SK2, and SK3, in the Adult Rat Central Nervous System. *Mol Cell Neurosci.* 15, 476–493.

Stocker, M., Krause, M., and Pedarzani, P. (1999). An apamin-sensitive Ca²⁺-activated K⁺ current in hippocampal pyramidal neurons. *Neurobiology* 96, 4662–4667.

Taschenberger, H., and von Gersdorff, H. (2000). Fine-tuning an auditory synapse for speed and fidelity: developmental changes in presynaptic waveform, EPSC kinetics, and synaptic plasticity. *J. Neurosci.* 20, 9162–9173.

Taschenberger, H., Leão, R.M., Rowland, K.C.K.C., Spirou, G.A.G.A., von Gersdorff, H., Auger, C., Kondo, S., Marty, A., Bellingham, M.C., Lim, R., et al. (2002). Optimizing Synaptic Architecture and Efficiency for High-Frequency Transmission. *Neuron* 36, 1127–1143.

Teder-Sälejärvi, W.A., Pierce, K.L., Courchesne, E., and Hillyard, S.A. (2005). Auditory spatial localization and attention deficits in autistic adults. *Cogn. Brain Res.* 23, 221–234.

Tritsch, N.X., Rodríguez-Contreras, A., Crins, T.T.H., Wang, H.C., Borst, J.G.G., and Bergles, D.E. (2010). Calcium action potentials in hair cells pattern auditory neuron activity before hearing onset. *Nat. Neurosci.* 13, 1050–1052.

Trussell, L.O. (1997). Cellular mechanisms for preservation of timing in central auditory pathways. *Curr. Opin. Neurobiol.* 7, 487–492.

Trussell, L.O. (1999). SYNAPTIC MECHANISMS FOR CODING TIMING IN AUDITORY NEURONS.

Vergara, C., Latorre, R., Marrion, N. V., and Adelman, J.P. (1998). Calcium-activated potassium channels. *Curr. Opin. Neurobiol.* 8, 321–329.

Visser, E., Zwiers, M.P., Kan, C.C., Hoekstra, L., van Opstal, A.J., and Buitelaar, J.K.

- (2013). Atypical vertical sound localization and sound-onset sensitivity in people with autism spectrum disorders. *J. Psychiatry Neurosci.* 38, 398–406.
- Wang, L.Y., and Kaczmarek, L.K. (1998). High-frequency firing helps replenish the readily releasable pool of synaptic vesicles. *Nature* 394, 384–388.
- Wang, L.-Y., Fedchyshyn, M.J., and Yang, Y.-M. (2009). Action potential evoked transmitter release in central synapses: insights from the developing calyx of Held. *Mol. Brain* 2, 36.
- Wang, L.Y., Gan, L., Forsythe, I.D., and Kaczmarek, L.K. (1998). Contribution of the Kv3.1 potassium channel to high frequency firing in mouse auditory neurones. *J. Physiol.* 509, 183–194.
- Wang, Q., Curran, M.E., Splawski, I., Burn, T.C., Millholland, J.M., VanRaay, T.J., Shen, J., Timothy, K.W., Vincent, G.M., de Jager, T., et al. (1996). Positional cloning of a novel potassium channel gene: KVLQT1 mutations cause cardiac arrhythmias. *Nat Genet* 12, 17–23.
- Wu, L.G., Borst, J.G., and Sakmann, B. (1998). R-type Ca²⁺ currents evoke transmitter release at a rat central synapse. *Proc. Natl. Acad. Sci. U. S. A.* 95, 4720–4725.
- Wu, L.G., Westenbroek, R.E., Borst, J.G., Catterall, W. a, and Sakmann, B. (1999). Calcium channel types with distinct presynaptic localization couple differentially to transmitter release in single calyx-type synapses. *J. Neurosci.* 19, 726–736.
- Wu, X.-S., McNeil, B.D., Xu, J., Fan, J., Xue, L., Melicoff, E., Adachi, R., Bai, L., and Wu, L.-G. (2009). Ca²⁺ and calmodulin initiate all forms of endocytosis during depolarization at a nerve terminal. *Nat. Neurosci.* 12, 1003–1010.
- Xia, X.M., Fakler, B., Rivard, a, Wayman, G., Johnson-Pais, T., Keen, J.E., Ishii, T., Hirschberg, B., Bond, C.T., Lutsenko, S., et al. (1998). Mechanism of calcium gating in small-conductance calcium-activated potassium channels. *Nature* 395, 503–507.

- Xu, J., Berret, E., and Kim, J.H. (2017). Activity-dependent formation and location of voltage-gated sodium channel clusters at a CNS nerve terminal during postnatal development. *J. Neurophysiol.* *117*, 582–593.
- Yang, Y.-M. (2006a). Amplitude and Kinetics of Action Potential-Evoked Ca²⁺ Current and Its Efficacy in Triggering Transmitter Release at the Developing Calyx of Held Synapse. *J. Neurosci.* *26*, 5698–5708.
- Yang, Y.-M. (2006b). Amplitude and Kinetics of Action Potential-Evoked Ca²⁺ Current and Its Efficacy in Triggering Transmitter Release at the Developing Calyx of Held Synapse. *J. Neurosci.* *26*, 5698–5708.
- Yang, Y.-M., Wang, W., Fedchyshyn, M.J., Zhou, Z., Ding, J., and Wang, L.-Y. (2014). Enhancing the fidelity of neurotransmission by activity-dependent facilitation of presynaptic potassium currents. *Nat. Commun.* *5*.
- Yue, C., and Yaari, Y. (2006). Axo-somatic and apical dendritic Kv7/M channels differentially regulate the intrinsic excitability of adult rat CA1 pyramidal cells. *J. Neurophysiol.* *95*, 3480–3495.
- Yus-Nájera, E., Muñoz, A., Salvador, N., Jensen, B.S., Rasmussen, H.B., Defelipe, J., and Villarroel, A. (2003). Localization of KCNQ5 in the normal and epileptic human temporal neocortex and hippocampal formation. *Neuroscience* *120*, 353–364.
- Zuberi, S.M., Eunson, L.H., Spauschus, A., De Silva, R., Tolmie, J., Wood, N.W., McWilliam, R.C., Stephenson, J.P.B., Kullmann, D.M., and Hanna, M.G. (1999). A novel mutation in the human voltage-gated potassium channel gene (Kv1.1) associates with episodic ataxia type 1 and sometimes with partial epilepsy. *Brain* *122*, 817–825.

BIOGRAPHY

Yihui Zhang was born in Anhui, China on April 19, 1989. In the fall of 2007, she entered School of Basic Medical Science at Southern Medical University in Guangzhou, China where she received her Bachelor of Medicine degree in 2012. She later entered the Cell and Molecular Department at Tulane University in New Orleans, Louisiana in fall of 2012 to pursue a Doctorate of Philosophy degree under the advisory of Dr. Hai Huang.